



PUBLISHED FOR SISSA BY SPRINGER

RECEIVED: May 15, 2016

REVISED: August 29, 2016

ACCEPTED: September 1, 2016

PUBLISHED: September 15, 2016

Two-loop master integrals for the mixed EW-QCD virtual corrections to Drell-Yan scattering

Roberto Bonciani,^a Stefano Di Vita,^b Pierpaolo Mastrolia^{c,d} and Ulrich Schubert^c

^a*Dipartimento di Fisica, Università di Roma “La Sapienza” and INFN Sezione Roma, Piazzale Aldo Moro 5, I-00185 Roma, Italy*

^b*DESY, Notkestraße 85, D-22607 Hamburg, Germany*

^c*Max-Planck-Institut für Physik, Föhringer Ring 6, D-80805 München, Germany*

^d*Dipartimento di Fisica e Astronomia, Università di Padova and INFN Sezione di Padova, Via Marzolo 8, I-35131 Padova, Italy*

E-mail: roberto.bonciani@roma1.infn.it, stefano.divita@desy.de, pierpaolo.mastrolia@cern.ch, schubert@mpp.mpg.de

ABSTRACT: We present the calculation of the master integrals needed for the two-loop QCD×EW corrections to $q + \bar{q} \rightarrow l^- + l^+$ and $q + \bar{q}' \rightarrow l^- + \bar{\nu}$, for massless external particles. We treat the W and Z bosons as degenerate in mass. We identify three types of diagrams, according to the presence of massive internal lines: the no-mass type, the one-mass type, and the two-mass type, where all massive propagators, when occurring, contain the same mass value. We find a basis of 49 master integrals and evaluate them with the method of the differential equations. The Magnus exponential is employed to choose a set of master integrals that obeys a canonical system of differential equations. Boundary conditions are found either by matching the solutions onto simpler integrals in special kinematic configurations, or by requiring the regularity of the solution at pseudothresholds. The canonical master integrals are finally given as Taylor series around $d = 4$ space-time dimensions, up to order four, with coefficients given in terms of iterated integrals, respectively up to weight four.

KEYWORDS: NLO Computations

ARXIV EPRINT: [1604.08581](https://arxiv.org/abs/1604.08581)

Contents

| | | |
|----------|---|-----------|
| 1 | Introduction | 1 |
| 2 | Notation and conventions | 5 |
| 3 | Systems of differential equations for master integrals | 8 |
| 3.1 | General solution | 9 |
| 3.2 | Properties of Chen’s iterated integrals | 11 |
| 3.3 | Mixed Chen-Goncharov representation | 12 |
| 3.4 | Constant Goncharov polylogarithms | 14 |
| 4 | One-mass master integrals | 14 |
| 4.1 | One-loop | 14 |
| 4.2 | Two-loop | 16 |
| 5 | Two-mass master integrals | 18 |
| 5.1 | One-loop | 18 |
| 5.2 | Two-loop | 21 |
| 6 | Conclusions | 24 |
| A | Variables for the one-mass and two-mass integrals | 25 |
| A.1 | One-mass type | 25 |
| A.2 | Two-mass type | 26 |
| A.2.1 | Range of values for w | 26 |
| A.2.2 | Range of values for z | 27 |
| B | Two-loop $d\log$-forms | 28 |
| B.1 | One-mass | 28 |
| B.2 | Two-mass | 32 |

1 Introduction

The Drell-Yan production of Z and W bosons [1] is one of the standard candles for physical studies at the LHC. Due to the big cross section and clean experimental signature, Drell-Yan processes can be measured with small experimental uncertainty and, therefore, allow for very precise tests of the Standard Model of fundamental interactions (SM). They give access to the determination of important parameters of the weak sector, as for instance the sine of the weak mixing angle and the W boson mass, that together with the top and the Higgs masses provides stringent constraints on the validity of the SM. Furthermore,

Drell-Yan processes constitute the SM background in searches of New Physics, involving for instance new vector boson resonances, Z' and W' , originating from GUT extensions of the SM. Finally, the Drell-Yan mechanism is used for constraining parton distribution functions, for the detector calibration, and for the determination of the collider luminosity. For all these reasons, an accurate and reliable experimental and theoretical control on Drell-Yan processes would be of the maximum importance for future physics studies at colliders.

The theoretical description of Drell-Yan processes currently includes NNLO QCD and NLO EW radiative corrections, implemented in flexible tools able to provide predictions for inclusive observables as well as kinematic distributions [2]. Current theoretical predictions are in good agreement with the experimental measurements. However, higher theoretical accuracy is needed in order to match the future experimental requirements, in particular in view of the run II of the LHC. A consistent part of the effort needed to increase the theoretical accuracy regards higher-order perturbative corrections.

Very recently, NNNLO QCD corrections were calculated for the Higgs total production cross section in gluon-gluon fusion [3, 4]. The residual factorization/renormalization scales variation moved from about 10-15% of the NNLO calculation (supplemented by NNLL resummation) to about 5% of the current result. These results will be applied to Drell-Yan as well, since they involve the evaluation of the same topologies for the calculation of the corresponding Feynman diagrams [5–10].

At the same order of accuracy (one can roughly think to exchange two powers of α_S with one power of α), the mixed EW-QCD corrections have to be taken into account. As in the case of QCD NNLO with EW NLO perturbative corrections, the mixed EW-QCD corrections are expected to become of similar size with respect to QCD NNNLO at high leptonic invariant mass [11].

At LO, the partonic process in the SM is mediated by the exchange of a photon or a Z/W vector boson, in the s annihilation channel: $q\bar{q} \rightarrow \gamma, Z \rightarrow l^-l^+$ and $q\bar{q} \rightarrow W \rightarrow l\nu$.

At higher orders in the coupling constants, we can distinguish between QCD and electroweak (EW) or mixed (EW-QCD) corrections to the LO process. In the first case, only the initial state receives quantum corrections, since the leptonic final state does not couple to gluons.

The NLO QCD corrections to the total cross section were calculated in [12, 13] and revealed a sizable increase of the cross section with respect to the LO result. The NNLO QCD corrections [14, 15] stabilized, then, the convergence of the perturbative series.

QCD fixed-order corrections to the total production cross section are supplemented by the resummation of soft-gluon logarithmically enhanced terms, up to NNNLL approximation [16–19].

EW quantum corrections allow exchanges of quanta between initial and final states. Therefore, already at the NLO, massive four-point functions have to be evaluated. Since the bulk of the corrections for inclusive observables comes from the resonant region, in which the exchanged vector boson is nearly on-shell, electroweak NLO corrections to the total cross section were calculated for the W [20] and Z [21] in narrow-width approximation.

More exclusive observables are known in the literature. The Z and W production at non-zero transverse momentum p_T is known at the NLO in QCD [22–27] and in the full

SM [28]. NLO corrections to the production of a vector boson with a jet were considered in [29–32]. The two-loop QCD helicity amplitudes for the production of a Z or a W with a photon have also been calculated [33]. For small p_T ($p_T \ll m_W, m_Z$) the convergence of the fixed-order calculation is spoiled by the large logarithmic terms $\alpha_S^n \log^m(m_W^2/p_T^2)$ that have to be resummed [34–44]. Finally, the rapidity distribution of a vector boson is known at the NNLO in QCD [45].

The NLO corrections are available in a fully differential description. They are implemented in flexible NLO Monte Carlo programs [46–52], and merged with QCD parton shower [53–56] in the MC@NLO [57] and POWHEG [58] frameworks.

Pure QED generators are also available [59–69]. Although these implementations provide an accurate description of the process and allow for realistic phenomenological studies at the hadronic level, they are not accurate enough for the performances of the run II at the LHC. The NNLO results mentioned above, however, are widely inclusive and they cannot provide realistic descriptions, that necessarily have to include experimental cuts. Therefore, a fully differential description of the Drell-Yan process at the NNLO is needed.

With this respect, the state of the art is represented by the two MC programs FEWZ [70, 71], that includes also EW NLO corrections [72], and DYNNLO [73, 74]. In these two programs, the decay products of the vector boson, the spin correlations and the finite-width effects are also taken into account.

Very recently, the merging of NNLO corrections with QCD parton shower was also considered [75–77].

A sizable impact on the $pp(\bar{p}) \rightarrow W \rightarrow l\nu$ distributions, and therefore on the determination of the W mass, comes from the QCD initial state radiation (ISR) with QED final state radiation (FSR) or from the real-virtual (factorizable) corrections. However, at the level of precision required ($\Delta m_W \sim 10$ MeV), the complete set of mixed EW-QCD corrections may be important and has to be considered.

The NNLO mixed EW-QCD corrections to the production of a leptonic pair, i.e. order $\alpha\alpha_S$ corrections to the LO partonic amplitude, consist of two-loop $2 \rightarrow 2$ processes, in which the quark-antiquark initial state goes in the final leptonic pair (l^+l^- or $l\nu$), one-loop $2 \rightarrow 3$ processes, in which the final leptonic pair is produced together with an unresolved photon or gluon, and tree-level $2 \rightarrow 4$ processes in which the leptonic pair is produced together with an unresolved photon and an unresolved gluon.

The QCD \times QED perturbative corrections were considered in [78]. In [79], the mixed two-loop corrections to the form factors for the production of a Z boson were calculated analytically, expressing the result in terms of harmonic polylogarithms and related generalizations. In [80], the authors calculated the mixed corrections in the pole approximation near the resonance region. In particular, they worked out in this region three different contributions. The first are the ones coming from the QCD corrections to the production process, which turned out to be suppressed below the percent level. Then, there is the photonic final state radiation, which is the dominant contribution. Finally, they considered the non-factorizable contributions, due to soft-photon exchange between the production and the decay processes. These last contributions are suppressed way below the percent level and they are negligible for the current phenomenological purposes. In [81], the mixed $\alpha\alpha_S$

contributions in the resonant region coming from factorizable initial-final corrections were fully exploited. These contributions represent the bulk of the corrections near resonance. The mixed $\alpha\alpha_S$ corrections worked out in the pole approximation are phenomenologically sufficient for a detailed description of the Drell-Yan processes near the resonance. However, in order both to further check this statement and to be able to treat the process also in physical regions different from the resonance, a complete diagrammatic calculation would be desirable.

In this article, we present the calculation of the master integrals (MIs) needed for the virtual corrections to the two-loop $2 \rightarrow 2$ processes:

$$q + \bar{q} \rightarrow l^- + l^+, \quad \text{and} \quad q + \bar{q}' \rightarrow l^- + \bar{\nu},$$

for massless external particles.

The Feynman diagrams contributing to the process $q + \bar{q} \rightarrow l^- + l^+$ can involve the exchange of up to two virtual massive vector bosons. However, they never contain W and Z propagators at the same time. As a consequence of that, the master integrals involved in the calculation contain at most two equal internal masses and therefore they depend three scales.

The situation is different for the diagrams contributing to the process $q + \bar{q}' \rightarrow l^- + \bar{\nu}$. In this case, double massive exchanges can occur with the two different bosons in the same Feynman diagram, and therefore one should evaluate master integrals depending on four different scales. However, the masses of the W and Z bosons are numerically close to each other; in fact $\Delta m^2 \equiv m_Z^2 - m_W^2 \ll m_Z^2$. Therefore, in the diagrams containing both Z and W propagators at the same time, one can perform a series expansion in $\xi \equiv \Delta m^2/m_Z^2 \sim 0.25$ reducing effectively the number of scales on which the corresponding masters depend to three. Within this approximation, all topologies appearing in the two-loop QCD \times EW virtual corrections to Drell-Yan scattering shall contain either no internal massive line, or one massive propagator, or two massive propagators with the same mass [82]. Should they be needed for achieving higher accuracy within the virtual amplitudes, the coefficients of the series in ξ correspond to scalar integrals with higher powers of the denominators.

Using the code **Reduze 2** [83, 84], the dimensionally regulated integrals involved in the calculation are reduced to a set of 49 MIs, which are later determined by means of the differential equations method [85–87], reviewed in [88, 89]. Of those 49 MIs, 8 contain only massless internal lines, 24 involve one massive line and 17 involve two massive lines. The system of differential equations obeyed by the MIs is cast in a canonical form [90], following the algorithm based on the use of the Magnus exponential, introduced in [91, 92].¹ Boundary conditions are retrieved either from the knowledge of simpler integrals emerging in specific kinematic limits, or by requiring the regularity of the solution at pseudothresholds.

Finally, the canonical MIs are given as Taylor series in ϵ ($= (4 - d)/2$), up to order ϵ^4 , d being the dimensional regularization parameter. The coefficients of the series are pure functions, represented as iterated integrals with rational and irrational kernels, up to weight four. The solution could in general be expressed in terms of Chen's iterated integrals. We

¹Other related studies can be found in [93–95].

actually adopt a *mixed representation*, where, when possible, we make explicit the presence of Goncharov polylogarithms (GPLs) [96, 97], also within the nested integration structure. This representation is suitable for the numerical evaluation of our solution.

While the two-loop four-point integrals with massless internal lines are well known in the literature [87, 98–100], the four point integrals with one and two massive internal lines considered here are new and represent the main result of this communication.

All the master integrals with the exception of 5 of them were cast in closed analytic form in terms of GPLs. Because of the presence of irreducible irrational weight functions, it has been necessary to cast 5 of the 17 MIs with two massive internal lines as one-dimensional integral formulas [101], involving GPLs in the integrands. The numerical evaluation of our solutions can, therefore, be performed with the help of the GiNaC library [102] for the evaluation of GPLs.

The article is structured as follows. Section 2 contains our notation and conventions. In section 3, we discuss the solution of canonical differential equations in terms of Chen’s iterated integrals. In section 4, we explicitly present the system of differential equations and the solutions for the one- and two-loop MIs that contain one massive propagator. In section 5, we give the system of differential equations for the one- and two-loop MIs containing two massive propagators, and we present the corresponding solutions. Conclusions are given in section 6. In appendix A, we discuss the kinematic domain of our analytic results. In appendix B, we give the coefficient matrices of the systems of differential equations in canonical form.

Our results are collected in ancillary files, available in the `arXiv` submission.

2 Notation and conventions

In this paper we study the two-loop corrections to the following partonic scattering processes:

$$q(p_1) + \bar{q}(p_2) \rightarrow l^-(p_3) + l^+(p_4), \quad (2.1)$$

$$q(p_1) + \bar{q}'(p_2) \rightarrow l^-(p_3) + \bar{\nu}(p_4). \quad (2.2)$$

The external particles are considered massless and on their mass-shell, $p_1^2 = p_2^2 = p_3^2 = p_4^2 = 0$. The scattering can be described in terms of the Mandelstam variables

$$s = (p_1 + p_2)^2, \quad t = (p_1 - p_3)^2, \quad u = (p_1 - p_4)^2, \quad (2.3)$$

in such a way that, due to momentum conservation, we have $s + t + u = 0$. The physical region is defined by

$$s > 0, \quad t = -\frac{s}{2}(1 - \cos \theta), \quad (2.4)$$

where θ is the scattering angle in the partonic center of mass frame, lying in the range $0 < \theta < \pi$. Therefore, while $s > 0$, t is always negative and $-s < t < 0$.

We calculate the quantum corrections to the processes in eqs. (2.1) and (2.2) using a Feynman-diagrammatic approach. After considering the interference with the leading order, and summing over the spins and colors, we express the squared absolute value of

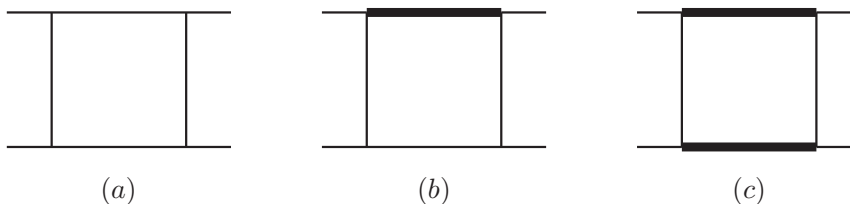


Figure 1. One-loop topologies. Thin lines represent massless external particles and propagators, while thick lines represent massive propagators.

the amplitude in terms of dimensionally regularized scalar integrals. These integrals are reduced to a set of MIs by means of integration-by-parts identities [103, 104] and Lorentz-invariance identities [87], implemented in the computer program² *Reduze 2* [83, 84].

The quantum corrections to the processes (2.1) and (2.2) can be expanded in power series of the coupling constants. At one loop, the QCD corrections consist of the exchange of a virtual gluon between the initial-state quarks. The final state is not affected, and at most massless three-point functions have to be evaluated. The EW corrections, instead, consist of the exchange of a photon, a Z boson or a W boson. Moreover, these quanta can be exchanged between the quarks in the initial state as well as between the leptons in the final state, but they can also be exchanged between a quark in the initial state and a lepton in the final state. Consequently, in the calculation of the one-loop corrections one has to evaluate massive box and vertex diagrams. In the process of $q\bar{q} \rightarrow l\nu$ one has to evaluate diagrams in which a Z and a W bosons are exchanged simultaneously. In order to reduce the number of scales present in the calculation, we perform a series expansion in the difference of the two squared masses. Expanding for instance the Z propagators around m_W , we find:

$$\frac{1}{p^2 - m_Z^2} = \frac{1}{p^2 - m_W^2 - \Delta m^2} \approx \frac{1}{p^2 - m_W^2} + \frac{m_Z^2}{(p^2 - m_W^2)^2} \xi + \dots \quad (2.5)$$

where

$$\xi = \frac{\Delta m^2}{m_Z^2} = \frac{m_Z^2 - m_W^2}{m_Z^2} \sim \frac{1}{4} \quad (2.6)$$

is the effective parameter of the expansion. The coefficients of the series in ξ are Feynman diagrams with equal masses, that therefore depend only on s , t , and the W mass, m_W . The expanded denominator will eventually appear with a power $\alpha > 1$. However, this does not cause any problem in the calculation, since diagrams with higher powers of the propagators are in any case reduced to the same set of MIs. For phenomenological purposes the first order in ξ might be sufficient, but in principle any order in ξ can be calculated without effort, just relying on the reduction procedure. We apply the same approximation to the two-loop diagrams as well.

At the one-loop level, the topologies involved in the QCD and EW corrections are shown in figure 1, where we distinguish: *a*) the massless case; *b*) the exchange of one massive particle; and *c*) the exchange of two massive particles.

²Other public programs are available for the reduction to the MIs [105–110].

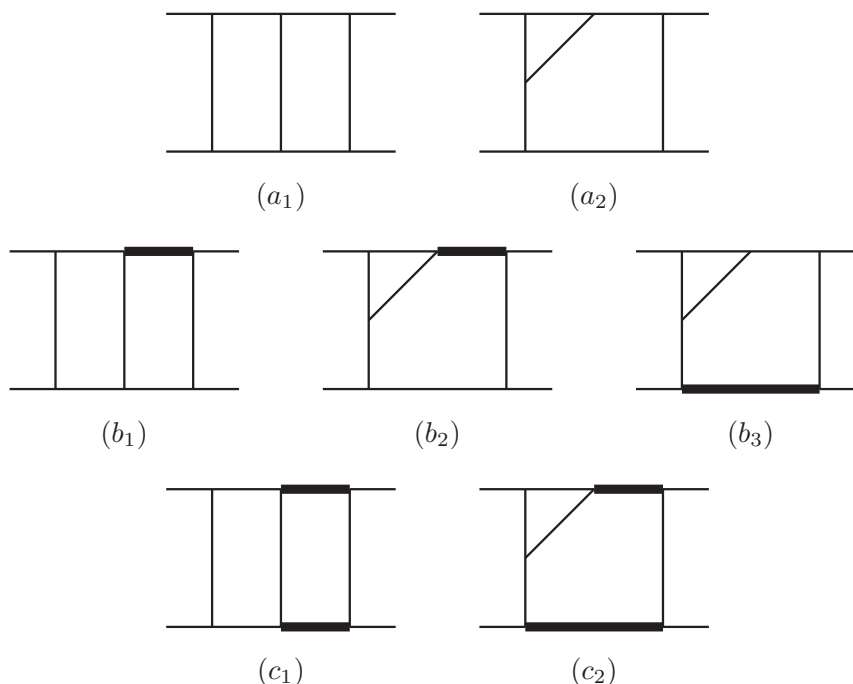


Figure 2. Two-loop topologies. Thin lines represent massless external particles and propagators, while thick lines represent massive propagators.

At the two-loop level, the topologies required by the $\mathcal{O}(\alpha\alpha_S)$ corrections are only planar. They are shown in figure 2. As for the one-loop case, we consider three classes of diagrams, according to the presence of massive particles. Topologies $a_1)$ and $a_2)$ belong to the same 9-denominators massless topology. They reduce to 8 MIs, that were already known in the literature [87, 98–100]. Topologies $b_1)$ – $b_3)$ have one massive propagator. They reduce to 31 MIs, out of which 24 contain one massive propagator and 7 are part of the MIs for topologies $a_1)$ and $a_2)$. The three-point functions were already known in the literature [111–113]. The four-point functions are calculated and presented here for the first time. Topologies $c_1)$ and $c_2)$ have two massive propagators and they reduce to 36 MIs, out of which 17 contain two massive propagators, 15 contain one massive propagator (and they are included in the set of MIs for topologies $b_1)$ – $b_3)$) and 4 contain only massless propagators. The three-point functions were known in the literature [114, 115] and the four-point functions are presented here for the first time.

The routings for one- and two-mass topologies, at the one- and two-loop level, can be defined in terms of the following sets of denominators D_n , where k_i ($i = 1, 2$) are the loop momenta, and p_i ($i = 1, \dots, 4$) are the external momenta:

- *One-mass topologies.* For the one-loop one-mass integrals (figure 1 b), we have:

$$D_1 = k_1^2, \quad D_2 = (k_1 - p_1)^2, \quad D_3 = (k_1 + p_2)^2 - m^2, \quad D_4 = (k_1 - p_1 + p_3)^2.$$

At two loops (figure 2 b_1 – b_3), instead, we have:

$$\begin{aligned} D_1 &= k_1^2, & D_2 &= k_2^2, & D_3 &= (k_1 + k_2)^2, & D_4 &= (k_1 - p_1)^2, \\ D_5 &= (k_1 + p_2)^2, & D_6 &= (k_1 + k_2 - p_1)^2 - m^2, & D_7 &= (k_1 + k_2 + p_2)^2, \\ D_8 &= (k_1 + k_2 - p_1 + p_3)^2, & D_9 &= (k_1 - p_1 + p_3)^2. \end{aligned} \quad (2.7)$$

- *Two-mass topologies.* For the one-loop two-mass integrals (figure 1 c), we have:

$$D_1 = k_1^2, \quad D_2 = (k_1 - p_1)^2 - m^2, \quad D_3 = (k_1 + p_2)^2 - m^2, \quad D_4 = (k_1 - p_1 + p_3)^2.$$

At two loops (figure 2 c_1 and c_2), instead, we have:

$$\begin{aligned} D_1 &= k_1^2, & D_2 &= k_2^2, & D_3 &= (k_1 + k_2)^2, & D_4 &= (k_1 - p_1)^2, \\ D_5 &= (k_1 + p_2)^2, & D_6 &= (k_1 + k_2 - p_1)^2 - m^2, & D_7 &= (k_1 + k_2 + p_2)^2 - m^2, \\ D_8 &= (k_1 + k_2 - p_1 + p_3)^2, & D_9 &= (k_1 - p_1 + p_3)^2. \end{aligned} \quad (2.8)$$

In the following we consider ℓ -loop Feynman integrals in d dimensions, built out of p of the above denominators, each raised to some integer power, of the form

$$\int \widetilde{d^d k_1} \dots \widetilde{d^d k_\ell} \frac{1}{D_{a_1}^{n_1} \dots D_{a_p}^{n_p}}, \quad (2.9)$$

where the integration measure is defined as

$$\widetilde{d^d k_i} \equiv \frac{d^d k_i}{(2\pi)^d} \left(\frac{i S_\epsilon}{16\pi^2} \right)^{-1} \left(\frac{m^2}{\mu^2} \right)^\epsilon, \quad (2.10)$$

with μ the 't Hooft scale of dimensional regularization, and

$$S_\epsilon \equiv (4\pi)^\epsilon \frac{\Gamma(1+\epsilon) \Gamma^2(1-\epsilon)}{\Gamma(1-2\epsilon)}. \quad (2.11)$$

In eqs. (2.10) and (2.11) we used $\epsilon = (4-d)/2$.

3 Systems of differential equations for master integrals

In this section, we describe the general structure of the systems of differential equations obeyed by the MIs, and the corresponding solutions. Sections dedicated to the one-mass and two-mass MIs will follow, where the details of their complete determination will be provided.

The b - and c -type MIs are functions of the Mandelstam invariants defined in eq. (2.3) and of the mass m . For their evaluation it is convenient to define the dimensionless ratios

$$x \equiv -\frac{s}{m^2}, \quad y \equiv -\frac{t}{m^2}, \quad z \equiv -\frac{u}{m^2}, \quad \text{with } x + y + z = 0. \quad (3.1)$$

The b -type and c -type MIs obey systems of partial differential equations in x and y , which can be combined into matrix equations for their total differentials. In general, the vector of MIs \mathbf{F} is solution of the following differential equation,

$$d\mathbf{F} = \mathbb{K} \mathbf{F}, \quad (3.2)$$

where the matrix \mathbb{K} depends *both* on the kinematic variables and on the spacetime dimension.

By means of a suitable basis transformation, built with the help of the *Magnus exponential* [91, 116] following the procedure outlined in section 2 of [92], we obtain a *canonical* set of MIs [90]. Such a basis obeys a system of differential equation where the dependence on ϵ is factorized from the kinematics. Moreover, the coefficient matrices can be assembled in a (logarithmic) differential form, referred to as canonical *dlog*-form. Hence, the canonical basis \mathbf{I} obeys the following system of equations,

$$d\mathbf{I} = \epsilon d\mathbb{A} \mathbf{I}, \quad (3.3)$$

with

$$d\mathbb{A} = \sum_{i=1}^n \mathbb{M}_i d\log \eta_i. \quad (3.4)$$

In eq. (3.4), $d\mathbb{A}$ is the *dlog* matrix written in terms of differentials $d\log \eta_i$, where $\eta_i = \eta_i(x, y)$ are functions of the kinematic variables, and coefficient matrices \mathbb{M}_i (with rational-number entries). The integrability conditions for eq. (3.3) read [90]

$$\partial_a \partial_b \mathbb{A} - \partial_b \partial_a \mathbb{A} = 0, \quad [\partial_a \mathbb{A}, \partial_b \mathbb{A}] = 0, \quad (3.5)$$

where $\partial_a \equiv \partial/\partial a$ and a and b are such that $a, b = x, y$ (i.e. ∂_a is the derivative with respect to one of the kinematic variables).

3.1 General solution

The general solution of the canonical system of differential equations (3.3) can be compactly written at a point $\vec{x} = (x^1, x^2) = (x, y)$ as

$$\mathbf{I}(\epsilon, \vec{x}) = \mathcal{P} \exp \left\{ \epsilon \int_{\gamma} d\mathbb{A} \right\} \mathbf{I}(\epsilon, \vec{x}_0), \quad (3.6)$$

where $\mathbf{I}(\epsilon, \vec{x}_0)$ is a vector of arbitrary constants, depending on ϵ , while $d\mathbb{A}$ depends only on the kinematic variables. In the above expression, the *path-ordered* exponential is a short notation for the series

$$\mathcal{P} \exp \left\{ \epsilon \int_{\gamma} d\mathbb{A} \right\} = \mathbb{1} + \epsilon \int_{\gamma} d\mathbb{A} + \epsilon^2 \int_{\gamma} d\mathbb{A} d\mathbb{A} + \epsilon^3 \int_{\gamma} d\mathbb{A} d\mathbb{A} d\mathbb{A} + \dots, \quad (3.7)$$

in which the line integral of the product of k matrix-valued 1-forms $d\mathbb{A}$ is understood in the sense of *Chen's iterated integrals* [117] (see also [118] and the pedagogical lectures [119]) and γ is a piecewise-smooth path

$$\gamma : [0, 1] \ni t \mapsto \gamma(t) = (\gamma^1(t), \gamma^2(t)), \quad (3.8)$$

such that $\gamma(0) = \vec{x}_0$ and $\gamma(1) = \vec{x}$. It follows from Chen's theorem that the iterated integrals in eq. (3.7) do not depend on the actual choice of the path, provided the curve does not contain any singularity of $d\mathbb{A}$ and it does not cross any of its branch cuts, but

only on the endpoints. In this sense, if one fixes \vec{x}_0 and lets \vec{x} vary, eq. (3.6) can be thought of as a function of \vec{x} . In the limit $\vec{x} \rightarrow \vec{x}_0$, the line shrinks to a point and all the path integrals in eq. (3.7) vanish, so that $\mathbf{I}(\epsilon, \vec{x}) \rightarrow \mathbf{I}(\epsilon, \vec{x}_0)$, i.e. the integration constants have a natural interpretation as *initial* values, and the path-ordered exponential as *evolution* operator. We assume that the vector of MIs at any point $\mathbf{I}(\vec{x})$ is normalized in such a way that it admits a Taylor series in ϵ :

$$\mathbf{I}(\epsilon, \vec{x}) = \mathbf{I}^{(0)}(\vec{x}) + \epsilon \mathbf{I}^{(1)}(\vec{x}) + \epsilon^2 \mathbf{I}^{(2)}(\vec{x}) + \dots \quad (3.9)$$

The solution $\mathbf{I}(\epsilon, \vec{x})$ is then in principle determined through (3.6) at any order of the ϵ -expansion, and reads (up to the coefficient of ϵ^4)

$$\mathbf{I}^{(0)}(\vec{x}) = \mathbf{I}^{(0)}(\vec{x}_0), \quad (3.10)$$

$$\mathbf{I}^{(1)}(\vec{x}) = \mathbf{I}^{(1)}(\vec{x}_0) + \int_{\gamma} d\mathbb{A} \mathbf{I}^{(0)}(\vec{x}_0), \quad (3.11)$$

$$\mathbf{I}^{(2)}(\vec{x}) = \mathbf{I}^{(2)}(\vec{x}_0) + \int_{\gamma} d\mathbb{A} \mathbf{I}^{(1)}(\vec{x}_0) + \int_{\gamma} d\mathbb{A} d\mathbb{A} \mathbf{I}^{(0)}(\vec{x}_0), \quad (3.12)$$

$$\begin{aligned} \mathbf{I}^{(3)}(\vec{x}) = & \mathbf{I}^{(3)}(\vec{x}_0) + \int_{\gamma} d\mathbb{A} \mathbf{I}^{(2)}(\vec{x}_0) + \int_{\gamma} d\mathbb{A} d\mathbb{A} \mathbf{I}^{(1)}(\vec{x}_0) \\ & + \int_{\gamma} d\mathbb{A} d\mathbb{A} d\mathbb{A} \mathbf{I}^{(0)}(\vec{x}_0), \end{aligned} \quad (3.13)$$

$$\begin{aligned} \mathbf{I}^{(4)}(\vec{x}) = & \mathbf{I}^{(4)}(\vec{x}_0) + \int_{\gamma} d\mathbb{A} \mathbf{I}^{(3)}(\vec{x}_0) + \int_{\gamma} d\mathbb{A} d\mathbb{A} \mathbf{I}^{(2)}(\vec{x}_0) \\ & + \int_{\gamma} d\mathbb{A} d\mathbb{A} d\mathbb{A} \mathbf{I}^{(1)}(\vec{x}_0) + \int_{\gamma} d\mathbb{A} d\mathbb{A} d\mathbb{A} d\mathbb{A} \mathbf{I}^{(0)}(\vec{x}_0). \end{aligned} \quad (3.14)$$

The problem of solving (3.3), given a set of initial conditions $\mathbf{I}(\epsilon, \vec{x}_0)$, reduces therefore to the evaluation of matrices of the type

$$\int_{\gamma} \underbrace{d\mathbb{A} \dots d\mathbb{A}}_{k \text{ times}}, \quad (3.15)$$

whose entries, due to (3.4), are linear combinations of Chen's iterated integrals of the form

$$\int_{\gamma} d\log \eta_{i_k} \dots d\log \eta_{i_1} \equiv \int_{0 \leq t_1 \leq \dots \leq t_k \leq 1} g_{i_k}^{\gamma}(t_k) \dots g_{i_1}^{\gamma}(t_1) dt_1 \dots dt_k, \quad (3.16)$$

with

$$g_i^{\gamma}(t) = \frac{d}{dt} \log \eta_i(\gamma(t)). \quad (3.17)$$

We refer to the number of iterated integrations k as the *weight* of the path-integral. The empty integral (eq. (3.16) for $k = 0$) is defined to be equal to 1. We stress that only the matrices (3.15) do not depend on the explicit choice of the path. The individual summands of the form in eq. (3.16), which contribute to their entries, in general depend on such a choice. To keep the notation compact, we define

$$\mathcal{C}_{i_k, \dots, i_1}^{[\gamma]} \equiv \int_{\gamma} d\log \eta_{i_k} \dots d\log \eta_{i_1}, \quad (3.18)$$

which also emphasizes that the iterated integrals in (3.16) are in general *functionals* of the path γ .

3.2 Properties of Chen's iterated integrals

The general theory of iterated path integrals was developed by Chen [117]. Chen's iterated integrals satisfy a number of properties that we summarize for completeness:

- *Invariance under path reparametrization.* The integral $\mathcal{C}_{i_k, \dots, i_1}^{[\gamma]}$ does not depend on how one chooses to parametrize the path γ .
- *Reverse path formula.* If the path γ^{-1} is the path γ traversed in the opposite direction, then

$$\mathcal{C}_{i_k, \dots, i_1}^{[\gamma^{-1}]} = (-1)^k \mathcal{C}_{i_k, \dots, i_1}^{[\gamma]}. \quad (3.19)$$

- *Recursive structure.* From (3.16) and (3.17) it follows that the line integral of one $d\log$ is defined as usual

$$\int_{\gamma} d\log \eta \equiv \int_{0 \leq t \leq 1} \frac{d\log \eta(\gamma(t))}{dt} dt, \quad (3.20)$$

and only depends on the endpoints \vec{x}_0, \vec{x}

$$\int_{\gamma} d\log \eta = \log \eta(\vec{x}) - \log \eta(\vec{x}_0). \quad (3.21)$$

It is convenient to introduce the path integral “up to some point along γ ”: given a path γ and a parameter $s \in [0, 1]$, one can define the 1-parameter family of paths

$$\gamma_s : [0, 1] \ni t \mapsto \gamma_s(t) = (\gamma^1(st), \gamma^2(st)). \quad (3.22)$$

If $s = 1$, then trivially $\gamma_s = \gamma$. If $s = 0$ the image of the interval $[0, 1]$ is just $\{\vec{x}_0\}$. If $s \in (0, 1)$, then the curve $\gamma_s([0, 1])$ starts at $\gamma(0) = \vec{x}_0$ and overlaps with the curve $\gamma([0, 1])$ up to the point $\gamma(s)$, where it ends. It is then easy to see that the path integral along γ_s can be written as

$$\mathcal{C}_{i_k, \dots, i_1}^{[\gamma_s]} = \int_{0 \leq t_1 \leq \dots \leq t_k \leq s} g_{i_k}^{\gamma}(t_k) \dots g_{i_1}^{\gamma}(t_1) dt_1 \dots dt_k, \quad (3.23)$$

which differs from eq. (3.16) by the fact that the outer integration (i.e. the one in dt_k) is performed over $[0, s]$ instead of $[0, 1]$. Having introduced γ_s , we can rewrite (3.16) in a recursive manner:

$$\mathcal{C}_{i_k, \dots, i_1}^{[\gamma]} = \int_0^1 g_{i_k}^{\gamma}(s) \mathcal{C}_{i_{k-1}, \dots, i_1}^{[\gamma_s]} ds. \quad (3.24)$$

From eq. (3.23) we can also immediately derive the following identity:

$$\frac{d}{ds} \mathcal{C}_{i_k, \dots, i_1}^{[\gamma_s]} = g_{i_k}^{\gamma}(s) \mathcal{C}_{i_{k-1}, \dots, i_1}^{[\gamma_s]}. \quad (3.25)$$

- *Shuffle algebra.* Chen's iterated integrals fulfill shuffle algebra relations: if $\vec{m} = m_M, \dots, m_1$ and $\vec{n} = n_N, \dots, n_1$ (with M and N natural numbers)

$$\mathcal{C}_{\vec{m}}^{[\gamma]} \mathcal{C}_{\vec{n}}^{[\gamma]} = \sum_{\text{shuffles } \sigma} \mathcal{C}_{\sigma(m_M), \dots, \sigma(m_1), \sigma(n_N), \dots, \sigma(n_1)}^{[\gamma]}, \quad (3.26)$$

where the sum runs over all the permutations σ that preserve the relative order of \vec{m} and \vec{n} .

- *Path composition formula.* If $\alpha, \beta : [0, 1] \rightarrow \mathcal{M}$ are such that $\alpha(0) = \vec{x}_0$, $\alpha(1) = \beta(0)$, and $\beta(1) = \vec{x}$, then the composed path $\gamma \equiv \alpha\beta$ is obtained by first traversing α and then β . One can prove that the integral over such a composed path satisfies

$$\mathcal{C}_{i_k, \dots, i_1}^{[\alpha\beta]} = \sum_{p=0}^k \mathcal{C}_{i_k, \dots, i_{p+1}}^{[\beta]} \mathcal{C}_{i_p, \dots, i_1}^{[\alpha]}. \quad (3.27)$$

- *Integration-by-parts formula.* In order to compute the path ordered integral of k $d\log$ forms using the definition, eq. (3.16) (or, equivalently, eq. (3.24)), in principle one would have to perform k nested integrations. When a fully analytic solution cannot be achieved, numerical integration can as well be employed. Therefore one can use an alternative form of the Chen iterated integral suitable for the combined use of analytic and numerical integrations. In fact, we observe that the innermost integration can always be performed analytically using (3.20), so that only $k - 1$ integrations are left. For instance, in the case $k = 2$,

$$\begin{aligned} \mathcal{C}_{b,a}^{[\gamma]} &= \int_0^1 g_b(t) \mathcal{C}_a^{[\gamma_t]} dt \\ &= \int_0^1 g_b(t) (\log \eta_a(\vec{x}(t)) - \log \eta_a(\vec{x}_0)) dt. \end{aligned} \quad (3.28)$$

For $k \geq 3$, one can proceed recursively using eq. (3.24), assuming that the numerical evaluation up to the first $k - 1$ iterations is a solved problem. Using integration by parts, one can show that the numerical integration over the outermost weight g_k can actually be avoided, leaving only $k - 2$ integrations to be performed

$$\mathcal{C}_{i_k, \dots, i_1}^{[\gamma]} = \log \eta_{i_k}(\vec{x}) \mathcal{C}_{i_{k-1}, \dots, i_1}^{[\gamma]} - \int_0^1 \log \eta_{i_k}(\vec{x}(t)) g_{i_{k-1}}(t) \mathcal{C}_{i_{k-2}, \dots, i_1}^{[\gamma_t]} dt. \quad (3.29)$$

3.3 Mixed Chen-Goncharov representation

In principle eq. (3.6) completely determines the solution, which can be written in terms of Chen's iterated integrals along an arbitrary piecewise-smooth path (see the discussion below eq. (3.6)). The initial conditions $\mathbf{I}(\vec{x}_0)$ can be computed analytically, if possible, or by means of numerical methods. The number of iterated integrals that have to be evaluated numerically can be minimized by the use of algebraic identities relating them. According to the discussion in section 3.2, the evaluation of the solution up to weight 4 requires in general 2 nested numerical integrations.

In order to obtain results that allow for an efficient numerical evaluation, we have chosen to give the solution in a mixed representation that involves GPLs and general Chen's iterated integrals. The representation in terms of GPLs is particularly convenient because public packages exist, like `GiNaC`, that implement their numerical evaluation in a fast and accurate way. Whenever the alphabet is rational in the kinematic variables x_i , one can always choose a path that allows to express the Chen iterated integrals in terms of GPLs, namely the broken line such that, in each segment, only one of the x_i is allowed

to vary. Along each segment, by means of factorization over the complex numbers, one can obtain a linear alphabet and, therefore, the GPLs representation. This approach is equivalent to integrating the differential equations for x and y separately. By integrating, say, the equation in x one obtains the solution in terms of GPLs of argument x up to an unknown function $\mathbf{H}(y)$. By taking the derivative with respect to y and matching to the equation in y , one obtains a differential equation for $\mathbf{H}(y)$. The latter can be again integrated in terms of GPLs of argument y , up to a constant.

As we will discuss in section 5, the alphabet for our differential equations is not always rational in the kinematic variables we use and, in that case, a representation in terms of GPLs cannot be given for the complete solution. To reach the mixed representation, we have exploited the property of path-independence of the coefficients of the ϵ -expansion of the solution eq. (3.6). In particular, eqs. (3.11)–(3.14) can be written in an equivalent alternative form using eq. (3.24):

$$\mathbf{I}^{(k)}(\vec{x}) = \mathbf{I}^{(k)}(\vec{x}_0) + \int_0^1 \left[\frac{d\mathbb{A}(t)}{dt} \mathbf{I}^{(k-1)}(\vec{x}_t) \right] dt, \quad (3.30)$$

where \vec{x}_t is the point $(x(t), y(t))$ along the curve identified by γ . We see that, in order to build the weight- k coefficient, one must perform a path integration over the weight- $(k-1)$ coefficient. The choice of such path is independent of the path used to compute the former because, as we have already discussed, each coefficient is a function of the sole endpoints. In other words, as far as the weight- k coefficient of the solution is concerned, we are free to choose the integration path independently for each of the k integrations (for each component of $\mathbf{I}(\vec{x})$).

To see how this can be useful in our computation, we note that the letters η_i (in suitable variables, say \vec{x}) can be grouped in two classes. The first contains the letters that are rational in the components of \vec{x} and happens to represent the alphabet for most of the MIs we need to compute. The second is the class of letters that are non-rational functions of the variables. The two classes together constitute the alphabet for the 5 most complicated MIs.

Starting from the weight-1 coefficient of the solution, we proceed as follows. As far as the involved η_i 's belong to the first class of letters, we can express the solution in terms of GPLs. We keep integrating in this manner until, at some weight k , the solution begins to involve non-rational η_i 's. At this point we proceed with the path integration as in (3.30). Within this approach, the weight $k-1$ solution is not expressed in terms of Chen's iterated integrals over an arbitrary path, but in terms of GPLs. We introduce the following notation to keep our results compact:

$$\mathcal{C}_{a|\vec{m}|\vec{n}}^{[\gamma]} \equiv \int_0^1 g_a^\gamma(t) G_{\vec{m}}^\gamma(x) G_{\vec{n}}^\gamma(y) dt, \quad (3.31)$$

$$\mathcal{C}_{a|\vec{m}|\emptyset}^{[\gamma]} \equiv \int_0^1 g_a^\gamma(t) G_{\vec{m}}^\gamma(x) dt, \quad (3.32)$$

$$\mathcal{C}_{a|\emptyset|\vec{n}}^{[\gamma]} \equiv \int_0^1 g_a^\gamma(t) G_{\vec{n}}^\gamma(y) dt, \quad (3.33)$$

$$\mathcal{C}_{a,\vec{b}|\vec{m}|\vec{n}}^{[\gamma]} \equiv \int_0^1 g_a^\gamma(t) \mathcal{C}_{\vec{b}|\vec{m}|\vec{n}}^{[\gamma_t]} dt, \quad (3.34)$$

where $G_{\vec{m}}^\gamma(x)$ and $G_{\vec{n}}^\gamma(y)$ stand for the GPLs $G_{\vec{m}}(x)$ and $G_{\vec{n}}(y)$ evaluated at $(x, y) = (\gamma^1(t), \gamma^2(t))$.

3.4 Constant Goncharov polylogarithms

In the determination of the boundary values of the MIs we encountered constant GPLs of argument 1 with weights drawn from three sets. For the one-mass MIs there is only one relevant set, with four weights,

- $\{-1, 0, \frac{1}{2}, 1\}$.

For the two-mass MIs we encountered the following two sets, with seven weights each

- $\{-1, 0, -i, i, 1, (-1)^{\frac{1}{3}}, -(-1)^{\frac{2}{3}}\}$,
- $\{-1, 0, -i, i, 1, -(-1)^{\frac{1}{6}}, -(-1)^{\frac{5}{6}}\}$,

where the former includes the third roots of -1 and the latter involves a subset of the sixth roots of -1 . With the help of **GiNaC**, we verified that, at order ϵ^k , the Taylor coefficient of each MI $I_i^{(k)}$ contains a combination of constant GPLs that turns out to be proportional to ζ_k , namely amounting to $q_{i,k} \zeta_k$, with $q_{i,k} \in \mathbb{Q}$. The resulting identities were verified at high numerical accuracy. As examples, we show,

$$0 = G_r + G_{-r^2}, \quad (3.35)$$

$$\begin{aligned} \zeta_2 = & 3G_{0,-r^2} + 4G_{r,-r^2} + 4G_{-r^2,0} - 2G_{-r^2,1} + 4G_{-r^2,r} \\ & + 4G_{-r^2,-r^2} + 3G_{0,r} + 4G_{r,0} - 2G_{r,1} + 4G_{r,r}, \end{aligned} \quad (3.36)$$

$$\begin{aligned} -\frac{77}{8}\zeta_3 = & G_{-1,-1,\frac{1}{2}} + G_{-1,\frac{1}{2},-1} + G_{-1,\frac{1}{2},1} + 3G_{0,0,\frac{1}{2}} + 3G_{0,\frac{1}{2},1} + G_{\frac{1}{2},-1,-1} \\ & + G_{\frac{1}{2},-1,1} - G_{\frac{1}{2},0,\frac{1}{2}} + 4G_{\frac{1}{2},0,1} + G_{\frac{1}{2},1,-1} + \frac{3}{2}\zeta_2 G_{\frac{1}{2}}, \end{aligned} \quad (3.37)$$

where for simplicity we omitted the argument ($x = 1$) of the GPLs and we defined the weight $r \equiv (-1)^{1/3}$. For related studies see also [120–123].

4 One-mass master integrals

In this section we describe the computation of the MIs with one internal massive line, namely topology (b) of figure 1 and topologies (b_1) – (b_3) of figure 2.

4.1 One-loop

The following set of MIs for the one-loop one-mass box obeys a differential equation in x and y , defined in eq. (3.1), which is linear in ϵ :

$$\begin{aligned} F_1 &= \epsilon \mathcal{T}_1, & F_2 &= \epsilon \mathcal{T}_2, & F_3 &= \epsilon \mathcal{T}_3, \\ F_4 &= \epsilon^2 \mathcal{T}_4, & F_5 &= \epsilon^2 \mathcal{T}_5. \end{aligned} \quad (4.1)$$

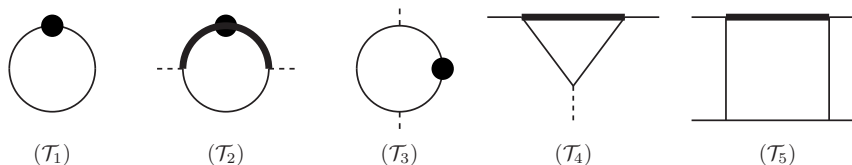


Figure 3. One-loop one-mass MIs $\mathcal{T}_{1,\dots,5}$. Thin lines represent massless external particles and propagators; thick lines stand for massive propagators; an horizontal (vertical) dashed external line represents an off-shell leg with squared momentum equal to s (t); dots indicate squared propagators.

where the \mathcal{T}_i are depicted in figure 3. By means of the Magnus exponential [91, 116], according to the procedure outlined in section 2 of [92], we obtain the canonical MIs

$$\begin{aligned} I_1 &= F_1, & I_2 &= -s F_2, & I_3 &= -t F_3, \\ I_4 &= -t F_4, & I_5 &= (s - m^2) t F_5. \end{aligned} \quad (4.2)$$

The alphabet of the corresponding $d\log$ -form, eq (3.4), is

$$\begin{aligned} \eta_1 &= x, & \eta_2 &= 1 + x, & \eta_3 &= y, \\ \eta_4 &= 1 - y, & \eta_5 &= x + y, \end{aligned} \quad (4.3)$$

and the coefficient matrices read

$$\begin{aligned} \mathbb{M}_1 &= \begin{pmatrix} 0 & 0 & 0 & 0 & 0 \\ 0 & 1 & 0 & 0 & 0 \\ 0 & 0 & 0 & 0 & 0 \\ 0 & 0 & 0 & 0 & 0 \\ 0 & 2 & -1 & -1 & 1 \end{pmatrix}, & \mathbb{M}_2 &= \begin{pmatrix} 0 & 0 & 0 & 0 & 0 \\ -1 & -2 & 0 & 0 & 0 \\ 0 & 0 & 0 & 0 & 0 \\ 0 & 0 & 0 & 0 & 0 \\ 0 & 0 & 0 & 0 & -2 \end{pmatrix}, & \mathbb{M}_3 &= \begin{pmatrix} 0 & 0 & 0 & 0 & 0 \\ 0 & 0 & 0 & 0 & 0 \\ 0 & 0 & -1 & 0 & 0 \\ 0 & 0 & 0 & 1 & 0 \\ 0 & 0 & 0 & 0 & -1 \end{pmatrix}, \\ \mathbb{M}_4 &= \begin{pmatrix} 0 & 0 & 0 & 0 & 0 \\ 0 & 0 & 0 & 0 & 0 \\ 0 & 0 & 0 & 0 & 0 \\ -1 & 0 & 1 & -1 & 0 \\ -1 & 0 & 1 & -1 & 0 \end{pmatrix}, & \mathbb{M}_5 &= \begin{pmatrix} 0 & 0 & 0 & 0 & 0 \\ 0 & 0 & 0 & 0 & 0 \\ 0 & 0 & 0 & 0 & 0 \\ 0 & 0 & 0 & 0 & 0 \\ 0 & -2 & -1 & 1 & 1 \end{pmatrix}. \end{aligned} \quad (4.4)$$

If $x > 0$ and $0 < y < 1$ all the letters η_i are positive. Since the alphabet is linear in x and y , according to the discussion in section 3.3, the solution can be conveniently cast in terms of GPLs. As a consequence, the analytic continuation to arbitrary complex values of x and y is straightforward, allowing the solution to be evaluated for any real and complex values of s , t , and m^2 . See appendix A for further details.

Instead of choosing a particular basepoint \vec{x}_0 , the integration constants of $I_{2\dots 5}$ can be easily fixed by demanding regularity at the pseudothresholds $t \rightarrow -m^2$, $u \rightarrow 0$, $s \rightarrow 0$ and their reality in the euclidean region. On the other hand, I_1 is a constant and must be determined by direct integration:

$$I_1 = \frac{\Gamma(1 - 2\epsilon)}{\Gamma(1 - \epsilon)^2}. \quad (4.5)$$

4.2 Two-loop

At the two-loop order, the following set of MIs admits ϵ -linear differential equations in x and y (defined in eq. (3.1)):

$$\begin{aligned}
 F_1 &= (1 - \epsilon)^2 \mathcal{T}_1, & F_2 &= \epsilon^2 \mathcal{T}_2, & F_3 &= \epsilon^2 \mathcal{T}_3, \\
 F_4 &= \epsilon^2 \mathcal{T}_4, & F_5 &= \epsilon^2 \mathcal{T}_5, & F_6 &= \epsilon^2 \mathcal{T}_6, \\
 F_7 &= \epsilon^3 \mathcal{T}_7, & F_8 &= \epsilon^3 \mathcal{T}_8, & F_9 &= \epsilon^3 \mathcal{T}_9, \\
 F_{10} &= \epsilon^2 \mathcal{T}_{10}, & F_{11} &= \epsilon^2 \mathcal{T}_{11}, & F_{12} &= \epsilon^3 \mathcal{T}_{12}, \\
 F_{13} &= \epsilon^4 \mathcal{T}_{13}, & F_{14} &= \epsilon^3 \mathcal{T}_{14}, & F_{15} &= \epsilon^4 \mathcal{T}_{15}, \\
 F_{16} &= \epsilon^3 \mathcal{T}_{16}, & F_{17} &= \epsilon^3 \mathcal{T}_{17}, & F_{18} &= \epsilon^4 \mathcal{T}_{18}, \\
 F_{19} &= \epsilon^3 \mathcal{T}_{19}, & F_{20} &= \epsilon^4 \mathcal{T}_{20}, & F_{21} &= \epsilon^3 \mathcal{T}_{21}, \\
 F_{22} &= \epsilon^4 \mathcal{T}_{22}, & F_{23} &= \epsilon^3 \mathcal{T}_{23}, & F_{24} &= (1 - 2\epsilon)\epsilon^3 \mathcal{T}_{24}, \\
 F_{25} &= \epsilon^3 \mathcal{T}_{25}, & F_{26} &= \epsilon^3 \mathcal{T}_{26}, & F_{27} &= \epsilon^4 \mathcal{T}_{27}, \\
 F_{28} &= \epsilon^3 \mathcal{T}_{28}, & F_{29} &= \epsilon^4 \mathcal{T}_{29}, & F_{30} &= \epsilon^4 \mathcal{T}_{30}, \\
 F_{31} &= \epsilon^4 \mathcal{T}_{31}, & & & &
 \end{aligned} \tag{4.6}$$

where the \mathcal{T}_i are depicted in figure 4. Once again, by means of Magnus exponentials, we are able to obtain a canonical basis:

$$\begin{aligned}
 I_1 &= F_1, & I_2 &= -s F_2, & I_3 &= 2m^2 F_2 + \lambda_- F_3, \\
 I_4 &= -s F_4, & I_5 &= -s F_5, & I_6 &= -t F_6, \\
 I_7 &= -s F_7, & I_8 &= -t F_8, & I_9 &= -s F_9, \\
 I_{10} &= \frac{m^2}{2\lambda_+} (2s\lambda_- F_{10} - 2F_1 - 3sF_5), & I_{11} &= s^2 F_{11}, & I_{12} &= -t F_{12}, \\
 I_{13} &= -s F_{13}, & I_{14} &= s^2 F_{14}, & I_{15} &= -s F_{15}, \\
 I_{16} &= s t F_{16}, & I_{17} &= s t F_{17}, & I_{18} &= -t F_{18}, \\
 I_{19} &= -m^2 t F_{19}, & I_{20} &= u F_{20}, & I_{21} &= -t \lambda_- F_{21}, \\
 I_{22} &= u F_{22}, & I_{23} &= -t \lambda_- F_{23}, & I_{24} &= -t F_{24}, \\
 I_{25} &= -t \lambda_- F_{25}, & I_{26} &= -t m^2 (F_{17} + \lambda_- F_{26}), & I_{27} &= s t F_{27}, \\
 I_{28} &= m^2 s ((m^2 + t) F_{28} - 2F_{27}), & I_{29} &= (s t + m^2 u) F_{29}, & I_{30} &= s t \lambda_- F_{30}, \\
 I_{31} &= m^2 s F_{29} - s \lambda_- F_{31}, & & & &
 \end{aligned} \tag{4.7}$$

where $\lambda_{\pm} = (m^2 \pm s)$. After combining the two differential equations into one total differential, we find a $d\log$ -form (3.4) with the alphabet

$$\begin{aligned}
 \eta_1 &= x, & \eta_2 &= 1 + x, & \eta_3 &= y, \\
 \eta_4 &= 1 - y, & \eta_5 &= x + y, & \eta_6 &= x + y + xy,
 \end{aligned} \tag{4.8}$$

which includes the additional letter η_6 as compared to one-loop (4.3). If $x > 0$ and $0 < y < 1$ all the letters η_i are positive. The coefficient matrices are given in the appendix (B.1). Since

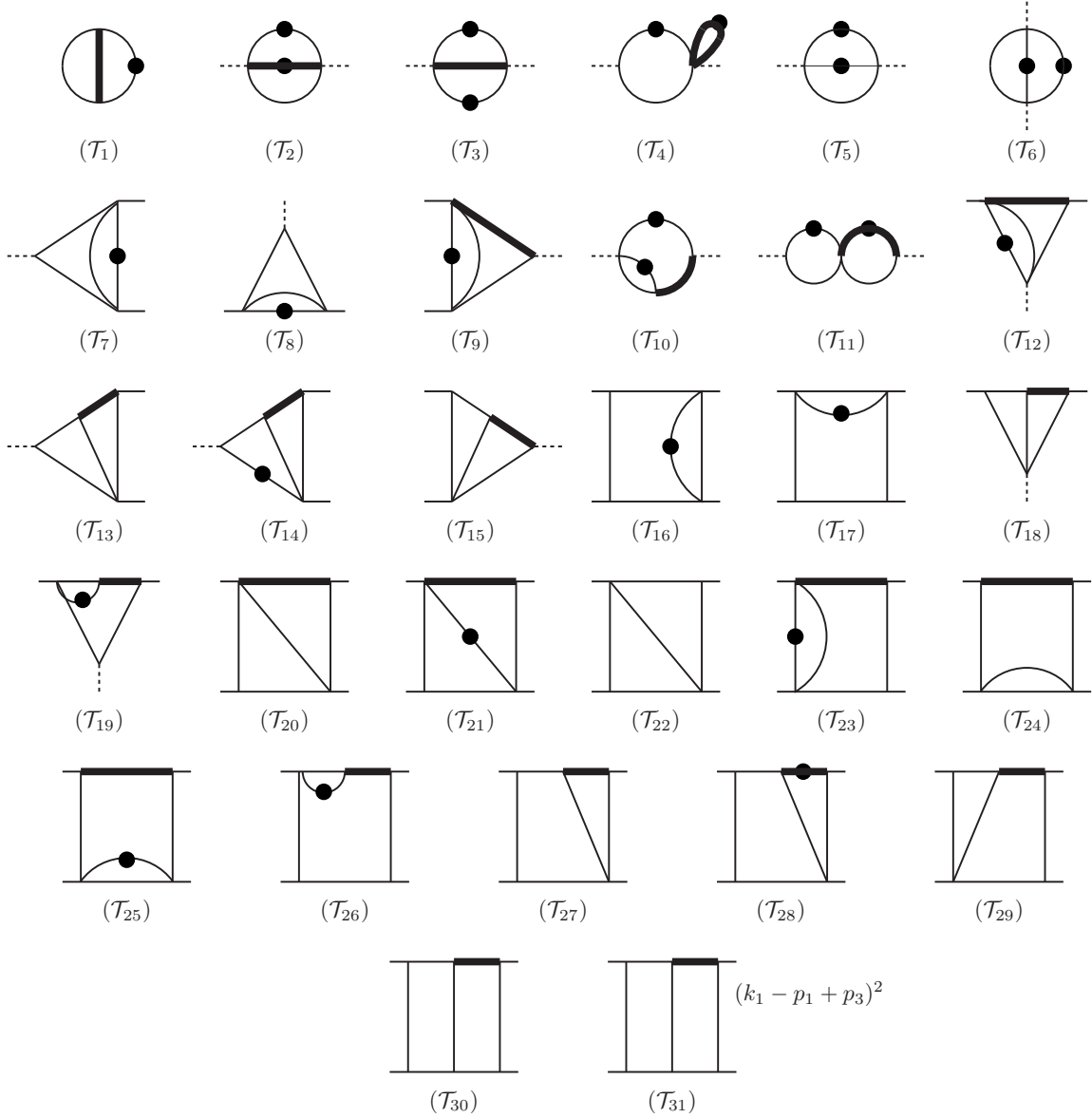


Figure 4. Two-loop one-mass MIs $\mathcal{T}_{1,\dots,31}$. The conventions are as in figure 3.

the additional letter is multilinear in x and y , also at the two-loop order we are able to obtain the solution in terms of GPLs (see the discussion in section 3.3).

We list the conditions imposed to the MIs for the determination of their boundary constants:

- regularity at $t \rightarrow -m^2$ and $u \rightarrow 0$ and imposing reality on the resulting boundary constants: $I_{2,\dots,5,7,\dots,10,12,14,\dots,17,19,\dots,31}$,
- limit $s \rightarrow 0$: $I_{11,13}$,
- limit $t \rightarrow 0$: I_{18} .

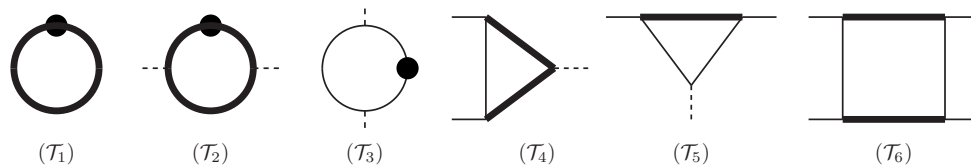


Figure 5. One-loop two-mass MIs $\mathcal{T}_{1,\dots,6}$. The conventions are as in figure 3.

This leaves us with $I_{1,6}$, to be determined by direct integration:

$$I_1 = -\frac{1}{2} \frac{\Gamma(1-2\epsilon)^2 \Gamma(1+2\epsilon)}{\Gamma(1-\epsilon)^3 \Gamma(1+\epsilon)}, \quad (4.9)$$

$$I_6 = -\frac{y^{-2\epsilon}}{\pi} \frac{\Gamma(\frac{1}{2}-\epsilon) \Gamma(\frac{1}{2}+\epsilon) \Gamma(1-2\epsilon)}{\Gamma(1-3\epsilon) \Gamma(1+\epsilon)}. \quad (4.10)$$

As in the one-loop case, owing to the explicit representation in terms of GPLs, the analytic continuation to arbitrary x and y is straightforward, so that all the one-mass MIs can be computed for any real and complex values of s , t , and m^2 (see appendix A). Our results have been successfully checked against **SecDec**, both in the Euclidean and in the physical regions.

The analytic expressions of all the MIs are explicitly given in electronic form in ancillary files that can be obtained from the **arXiv** version of this paper.

5 Two-mass master integrals

In this section we describe the computation of the MIs with two internal massive lines, namely topology (c) of figure 1 and topologies (c₁)-(c₂) of figure 2.

5.1 One-loop

We choose the following set of MIs, admitting a differential equation linear in ϵ

$$\begin{aligned} F_1 &= \epsilon \mathcal{T}_1, & F_2 &= \epsilon \mathcal{T}_2, & F_3 &= \epsilon \mathcal{T}_3, \\ F_4 &= \epsilon^2 \mathcal{T}_4, & F_5 &= \epsilon^2 \mathcal{T}_5, & F_6 &= \epsilon^2 \mathcal{T}_6, \end{aligned} \quad (5.1)$$

where the \mathcal{T}_i are shown in figure 5. After applying the Magnus transformation we obtain the following canonical basis

$$\begin{aligned} I_1 &= F_1, & I_2 &= -s \sqrt{1 - \frac{4m^2}{s}} F_2, & I_3 &= -t F_3, \\ I_4 &= -s F_4, & I_5 &= -t F_5, & I_6 &= s t \sqrt{1 - 4 \frac{m^2}{s} \left(1 + \frac{m^2}{t}\right)} F_6, \end{aligned} \quad (5.2)$$

The alphabet of the corresponding canonical $d\log$ -form, (3.4), is non-rational in s, t and m . In particular four square roots appear

$$\sqrt{-s}, \sqrt{4m^2 - s}, \sqrt{-t}, \text{ and } \sqrt{1 - \frac{4m^2}{s} \left(1 + \frac{m^2}{t}\right)}. \quad (5.3)$$

The alphabet can be rationalized through the change of variables

$$-\frac{s}{m^2} = \frac{(1-w)^2}{w}, \quad -\frac{t}{m^2} = \frac{w(1+z)^2}{z(1+w)^2}. \quad (5.4)$$

We note that the above mapping is not invertible at $s = 4m^2$. In terms of w and z , the alphabet reads

$$\begin{aligned} \eta_1 &= z, & \eta_2 &= 1+z, & \eta_3 &= 1-z, \\ \eta_4 &= w, & \eta_5 &= 1+w, & \eta_6 &= 1-w, \\ \eta_7 &= z-w, & \eta_8 &= z+w^2, & \eta_9 &= 1-wz, \\ \eta_{10} &= 1+w^2z, \end{aligned} \quad (5.5)$$

and the coefficient matrices are

$$\begin{aligned} \mathbb{M}_1 &= \begin{pmatrix} 0 & 0 & 0 & 0 & 0 & 0 \\ 0 & 0 & 0 & 0 & 0 & 0 \\ 0 & 0 & 1 & 0 & 0 & 0 \\ 0 & 0 & 0 & 0 & 0 & 0 \\ 1 & 0 & -1 & 0 & 0 & 0 \\ 0 & 2 & 0 & 0 & 0 & 0 \end{pmatrix}, & \mathbb{M}_4 &= \begin{pmatrix} 0 & 0 & 0 & 0 & 0 & 0 \\ 1 & 1 & 0 & 0 & 0 & 0 \\ 0 & 0 & -1 & 0 & 0 & 0 \\ 0 & -2 & 0 & -1 & 0 & 0 \\ 0 & 0 & 0 & 0 & 1 & 0 \\ 0 & 0 & 0 & 0 & 0 & -1 \end{pmatrix}, & \mathbb{M}_5 &= \begin{pmatrix} 0 & 0 & 0 & 0 & 0 & 0 \\ 0 & -2 & 0 & 0 & 0 & 0 \\ 0 & 0 & 2 & 0 & 0 & 0 \\ 0 & 0 & 0 & 0 & 0 & 0 \\ 2 & 0 & -2 & 0 & 0 & 0 \\ 0 & 0 & 0 & 0 & 0 & -2 \end{pmatrix}, & \mathbb{M}_7 &= \begin{pmatrix} 0 & 0 & 0 & 0 & 0 & 0 \\ 0 & 0 & 0 & 0 & 0 & 0 \\ 0 & 0 & 0 & 0 & 0 & 0 \\ 0 & 0 & 0 & 0 & 0 & 0 \\ -1 & 0 & 1 & 0 & -1 & 0 \\ -2 & 0 & 2 & 0 & -2 & 0 \end{pmatrix}, \\ \mathbb{M}_8 &= \begin{pmatrix} 0 & 0 & 0 & 0 & 0 & 0 \\ 0 & 0 & 0 & 0 & 0 & 0 \\ 0 & 0 & 0 & 0 & 0 & 0 \\ 0 & 0 & 0 & 0 & 0 & 0 \\ 0 & 0 & 0 & 0 & 0 & 0 \\ 0 & 0 & 0 & 2 & 2 & 1 \end{pmatrix}, & \mathbb{M}_9 &= \begin{pmatrix} 0 & 0 & 0 & 0 & 0 & 0 \\ 0 & 0 & 0 & 0 & 0 & 0 \\ 0 & 0 & 0 & 0 & 0 & 0 \\ 0 & 0 & 0 & 0 & 0 & 0 \\ -1 & 0 & 1 & 0 & -1 & 0 \\ 2 & 0 & -2 & 0 & 2 & 1 \end{pmatrix}, & \mathbb{M}_{10} &= \begin{pmatrix} 0 & 0 & 0 & 0 & 0 & 0 \\ 0 & 0 & 0 & 0 & 0 & 0 \\ 0 & 0 & 0 & 0 & 0 & 0 \\ 0 & 0 & 0 & 0 & 0 & 0 \\ 0 & 0 & 0 & 0 & 0 & 0 \\ 0 & 0 & 0 & -2 & -2 & 1 \end{pmatrix}, \end{aligned} \quad (5.6)$$

and $(\mathbb{M}_2)_{3,3} = -2$ and $(\mathbb{M}_2)_{5,5} = 2$ are the only non-vanishing entries in \mathbb{M}_2 , $(\mathbb{M}_3)_{6,6} = -2$ is the only non-vanishing entry in \mathbb{M}_3 , and $(\mathbb{M}_6)_{4,4} = 2$ is the only non-vanishing entry in \mathbb{M}_6 . In the region $0 < w < z < 1$ all the letters η_i are positive. The alphabet in (5.5) is linear in z but contains letters quadratic in w . As the latter can be linearized by factorization over the complex numbers, we are once again able to express the solution in terms of GPLs (see the discussion in section 3.3). As already discussed in section 5 for the one-mass case, owing to the explicit representation in terms of GPLs, the analytic continuation to any w and z is straightforward, so that all the one-loop two-mass MIs can be computed for arbitrary real and complex values of s , t , and m^2 (except for $s = 4m^2$). For a detailed discussion of how the regions in the real s, t plane are mapped to the $\mathbb{C} \times \mathbb{C}$ space of the w, z variables, see appendix A.

The integration constants of $I_{4,5,6}$ can be fixed by requiring their regularity at the pseudothresholds $s \rightarrow 0$, $t \rightarrow -m^2$ and $u \rightarrow 0$. The boundary constant of I_2 can be fixed by taking the $s \rightarrow 0$ limit. This leaves us with two integrals, $I_{1,3}$, to be determined by direct integration:

$$I_1 = \frac{\Gamma(1-2\epsilon)}{\Gamma(1-\epsilon)^2}, \quad (5.7)$$

$$I_3 = \left[\frac{z(1+w)^2}{w(1+z)^2} \right]^\epsilon. \quad (5.8)$$

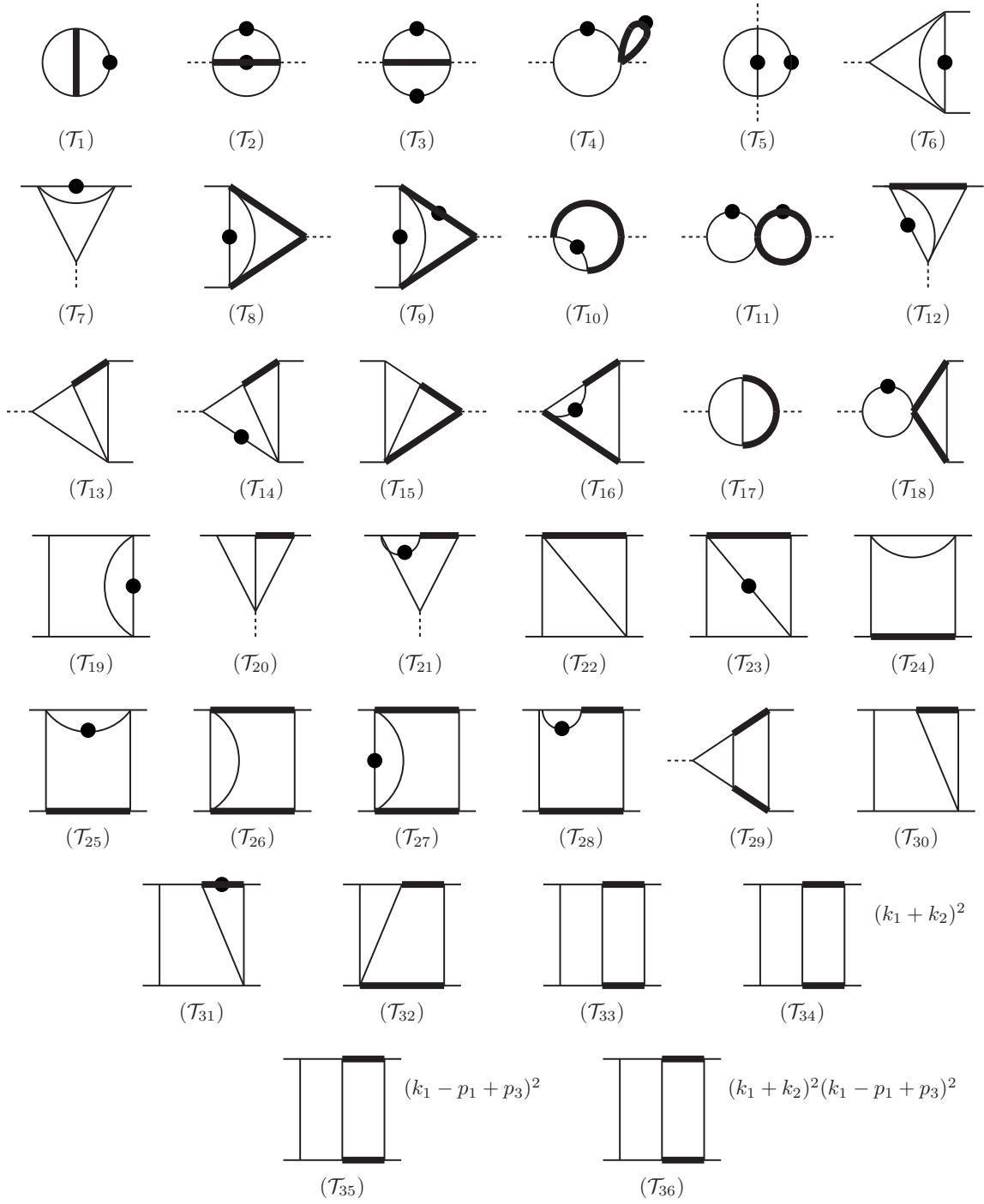


Figure 6. Two-loop two-mass MIs $\mathcal{T}_{1,\dots,36}$. The conventions are as in figure 3.

5.2 Two-loop

At the two-loop order we start with the set of MIs

$$\begin{aligned}
 F_1 &= (1 - \epsilon) \epsilon^2 \mathcal{T}_1, & F_2 &= \epsilon^2 \mathcal{T}_2, & F_3 &= \epsilon^2 \mathcal{T}_3, \\
 F_4 &= \epsilon^2 \mathcal{T}_4, & F_5 &= \epsilon^2 \mathcal{T}_5, & F_6 &= \epsilon^3 \mathcal{T}_6, \\
 F_7 &= \epsilon^3 \mathcal{T}_7, & F_8 &= \epsilon^3 \mathcal{T}_8, & F_9 &= \epsilon^2 \mathcal{T}_9, \\
 F_{10} &= (1 - 2\epsilon) \epsilon^2 \mathcal{T}_{10}, & F_{11} &= \epsilon^2 \mathcal{T}_{11}, & F_{12} &= \epsilon^3 \mathcal{T}_{12}, \\
 F_{13} &= \epsilon^4 \mathcal{T}_{13}, & F_{14} &= \epsilon^3 \mathcal{T}_{14}, & F_{15} &= \epsilon^4 \mathcal{T}_{15}, \\
 F_{16} &= \epsilon^3 \mathcal{T}_{16}, & F_{17} &= (1 - 2\epsilon) \epsilon^3 \mathcal{T}_{17}, & F_{18} &= \epsilon^3 \mathcal{T}_{18}, \\
 F_{19} &= \epsilon^3 \mathcal{T}_{19}, & F_{20} &= \epsilon^4 \mathcal{T}_{20}, & F_{21} &= \epsilon^3 \mathcal{T}_{21}, \\
 F_{22} &= \epsilon^4 \mathcal{T}_{22}, & F_{23} &= \epsilon^3 \mathcal{T}_{23}, & F_{24} &= (1 - 2\epsilon) \epsilon^3 \mathcal{T}_{24}, \\
 F_{25} &= \epsilon^3 \mathcal{T}_{25}, & F_{26} &= (1 - 2\epsilon) \epsilon^3 \mathcal{T}_{26}, & F_{27} &= \epsilon^3 \mathcal{T}_{27}, \\
 F_{28} &= \epsilon^3 \mathcal{T}_{28}, & F_{29} &= \epsilon^4 \mathcal{T}_{29}, & F_{30} &= \epsilon^4 \mathcal{T}_{30}, \\
 F_{31} &= \epsilon^3 \mathcal{T}_{31}, & F_{32} &= \epsilon^4 \mathcal{T}_{32}, & F_{33} &= \epsilon^4 \mathcal{T}_{33}, \\
 F_{34} &= \epsilon^4 \mathcal{T}_{34}, & F_{35} &= \epsilon^4 \mathcal{T}_{35}, & F_{36} &= \epsilon^4 \mathcal{T}_{36},
 \end{aligned} \tag{5.9}$$

where the \mathcal{T}_i are shown in figure 6. The MIs \mathbf{F} admit ϵ -linear differential equations, except for one of them. We have indeed

$$d\mathbf{F} = \mathbb{K} \mathbf{F}, \quad \mathbb{K} = \mathbb{K}_0 + \epsilon \mathbb{K}_1 + \frac{1}{1 - 2\epsilon} \mathbb{K}_2, \tag{5.10}$$

where $\mathbb{K}_0, \mathbb{K}_1$ and \mathbb{K}_2 do not depend on ϵ , and \mathbb{K}_2 is non-vanishing only in the inhomogeneous part of the differential equation for F_{36} . In a first step we apply the Magnus algorithm on $\mathbb{K}_0 + \epsilon \mathbb{K}_1$ in order to remove \mathbb{K}_0 , and in a second step we apply an ad-hoc transformation in order to remove the remaining non-linear piece.

The corresponding canonical basis reads

$$\begin{aligned}
 I_1 &= F_1, & I_2 &= -s F_2, & I_3 &= m^2 (2 F_2 + F_3) - s F_3, & I_4 &= -s F_4, \\
 I_5 &= -t F_5, & I_6 &= -s F_6, & I_7 &= -t F_7, & I_8 &= -s F_8, \\
 I_9 &= -\sqrt{1 - \frac{4m^2}{s}} \left(\frac{3}{2} F_8 + m^2 F_9 \right) - \frac{3}{2} s F_8, \\
 I_{10} &= \frac{1}{4} \left(1 + \sqrt{\frac{-s}{4m^2 - s}} \right) \left(-2F_1 + (m^2 - s) (F_2 + F_3) + m^2 F_2 \right. \\
 &\quad \left. + s F_{10} - s \sqrt{1 - \frac{4m^2}{s}} (F_2 + F_{10}) \right), \\
 I_{11} &= s^2 \sqrt{1 - \frac{4m^2}{s}} F_{11}, & I_{12} &= -t F_{12}, & I_{13} &= -s F_{13}, \\
 I_{14} &= s^2 F_{14}, & I_{15} &= -s F_{15}, & I_{16} &= -m^2 s F_{16}, \\
 I_{17} &= -s F_{17}, & I_{18} &= s^2 F_{18}, & I_{19} &= s t F_{19}, \\
 I_{20} &= -t F_{20}, & I_{21} &= -m^2 t F_{21}, & I_{22} &= u F_{22}, \\
 I_{23} &= (s - m^2) t F_{23}, & I_{24} &= -t F_{24}, & I_{25} &= (s - m^2) t F_{25},
 \end{aligned}$$

$$\begin{aligned}
 I_{26} &= -s F_{26}, & I_{27} &= s t \sqrt{1 - \frac{4m^2}{s} \left(1 + \frac{m^2}{t}\right)} F_{27}, \\
 I_{28} &= s t \sqrt{1 - \frac{4m^2}{s} \left(1 + \frac{m^2}{t}\right)} (F_{25} + m^2 F_{28}) + t(m^2 - s) F_{25}, \\
 I_{29} &= s^2 \sqrt{1 - \frac{4m^2}{s}} F_{29}, & I_{30} &= s t F_{30}, \\
 I_{31} &= -m^2 s (2F_{30} + (m^2 + t) F_{31}), & I_{32} &= s t \sqrt{1 + \frac{m^4}{t^2} - \frac{2m^2}{s} \left(1 - \frac{u}{t}\right)} F_{32}, \\
 I_{33} &= -s^2 t \sqrt{1 - \frac{4m^2}{s} \left(1 + \frac{m^2}{t}\right)} F_{33}, & I_{34} &= s^2 F_{34}, \\
 I_{35} &= s \sqrt{1 - \frac{4m^2}{s}} (2t F_{32} - s t F_{33} + s F_{35}) - s^2 t \sqrt{1 + \frac{4m^2}{s} \left(1 + \frac{m^2}{t}\right)} F_{33}, \\
 I_{36} &= \frac{s}{2(1-2\epsilon)} F_{17} - s t \left(1 - \sqrt{1 - \frac{4m^2}{s}}\right) F_{32} - s t F_{18} - 2t F_{22} \\
 &\quad - \frac{2m^2 s}{2 - \frac{s}{m^2} (1 - \sqrt{1 - \frac{4m^2}{s}})} (F_{29} + t F_{33} - F_{35}) - s F_{36}.
 \end{aligned} \tag{5.11}$$

As compared to the one-loop case (5.3) we encounter one additional square root in the canonical $d\log$ -form

$$\sqrt{1 + \frac{m^4}{t^2} - \frac{2m^2}{s} \left(1 - \frac{u}{t}\right)}, \tag{5.12}$$

which prevents the alphabet from being rationalized by the change of variables in eq. (5.4). In terms of w and z , the alphabet reads

$$\begin{aligned}
 \eta_1 &= z, & \eta_2 &= 1 + z, & \eta_3 &= 1 - z, \\
 \eta_4 &= w, & \eta_5 &= 1 + w, & \eta_6 &= 1 - w, \\
 \eta_7 &= 1 - w + w^2, & \eta_8 &= 1 - w z, & \eta_9 &= z - w, \\
 \eta_{10} &= 1 + w^2 z, & \eta_{11} &= z + w^2, \\
 \eta_{12} &= 4(1+z)^4 w^3 + (1-w)^2 \kappa_+^2(w, z), & \eta_{13} &= (1+w)\sqrt{\rho} + (1-w)\kappa_-(w, z), \\
 \eta_{14} &= (1+w)\sqrt{\rho} - (1-w)\kappa_-(w, z), & \eta_{15} &= (1+w)\sqrt{\rho} + (1-w)\kappa_+(w, z), \\
 \eta_{16} &= \frac{c_1 + c_2 \sqrt{\rho}}{c_3 + c_4 \sqrt{\rho}}, \\
 \eta_{17} &= 2(1-w)^2 w z^2 + \kappa_-^2(-w, z) + (z+w)(1+wz)\sqrt{\rho},
 \end{aligned} \tag{5.13}$$

where

$$\kappa_{\pm}(a, b) \equiv a(1+b)^2 \pm b(1+a)^2, \tag{5.14}$$

the argument of the square root entering $\eta_{13,\dots,17}$ is

$$\rho = 4wz^2(1+w)^2 - \kappa_+(w, z)\kappa_+(-w, -z), \tag{5.15}$$

and the four coefficients in η_{16} are given by

$$c_1 = (1+w)^2 (1-4w+w^2) z^2 (1+z)^2 + w^2 (1+z)^6 + 2w (1-w+w^2) z (1+z)^4 - 2(1+w)^4 z^3, \quad (5.16)$$

$$c_2 = (1-z^2) \kappa_+(w, z), \quad (5.17)$$

$$\begin{aligned} c_3 = & 2w^8 z^4 + 2w^7 z^3 (z^2 + 6z + 1) - w^6 (z-1)^2 z^2 (z^2 + 4z + 1) \\ & - 2w^5 z (z^6 - z^5 - 8z^4 - 8z^3 - 8z^2 - z + 1) \\ & + w^4 (z^8 - 2z^7 - 2z^6 + 6z^5 - 10z^4 + 6z^3 - 2z^2 - 2z + 1) \\ & - 2w^3 z (z^6 - z^5 - 8z^4 - 8z^3 - 8z^2 - z + 1) \\ & - w^2 (z-1)^2 z^2 (z^2 + 4z + 1) + 2wz^3 (z^2 + 6z + 1) + 2z^4, \end{aligned} \quad (5.18)$$

$$c_4 = -w(1-z^2)(z-w)(1-wz) \left(\kappa_-(-w, -z) + (1+w)^2 z \right). \quad (5.19)$$

In the region $0 < w < z < 1$ all the letters η_i are positive.

As already stressed, the alphabet is not rational in w and z . This prevents us from expressing the complete solution in terms of GPLs. In particular, the structure of the coefficient matrices \mathbb{M}_i is such that the solution for $I_{32}^{(3)}$ and for $I_{32,\dots,36}^{(4)}$, see eqs. (3.13), (3.14), involves path integration over $d\log$'s with non rational arguments. Nevertheless, the MIs $I_{1,\dots,31}$ admit a representation in terms of GPLs which is convenient for their numerical evaluation. As for the remaining MIs, we followed the procedure outlined in section 3.3: we express the solution up to weight 2 for I_{32} and up to weight 3 for $I_{33,\dots,36}$ in terms of GPLs and then obtain an 1-fold integral representation for the higher weights (for $I_{32,\dots,36}^{(4)}$ we use eq. (3.29)).

We list the conditions imposed to integrals $I_{1,\dots,31}$ for the determination of their boundary constants:

- independent input: $I_{1,4,\dots,7,13,14,20,25}$,
- regularity at $s \rightarrow 0$: I_{24} ,
- regularity at $t \rightarrow -m^2$: $I_{12,21}$,
- regularity at $u \rightarrow 0$: $I_{19,30,31}$,
- limit $s \rightarrow 0$: $I_{2,3,6,\dots,10,15,\dots,18,29}$,
- limit $t \rightarrow -m^2$ and $s \rightarrow 0$: I_{28} ,
- regularity at $s \rightarrow 0$ and matching to independent input: $I_{22,23}$.

For the MIs $I_{32,\dots,36}$ we observe that regularity at $u = s = t = 0$, corresponding to $\vec{x}_0 = (w_0, z_0) = (1, -1)$, implies

$$I_{32,\dots,36}(\epsilon, \vec{x}_0) = 0, \quad (5.20)$$

that we choose as initial condition of our solution in terms of iterated integrals.

The MIs $I_{1,\dots,31}$ are represented in terms of GPLs. As already discussed for the one-loop case, for such MIs the analytic continuation to arbitrary w and z is straightforward.

Therefore the MIs $I_{1,\dots,31}$ can be computed for any real and complex values of s , t , and m^2 (except for $s = 4m^2$, see appendix A for further comments). We checked our results in the Euclidean and physical regions against **SecDec** finding complete agreement.

The explicit evaluation of $I_{32,\dots,36}$ requires a careful choice of the integration path, in such a way that no branch cuts are crossed. We successfully checked our results in the Euclidean region $s < 0$ (see appendix A) against the numerical values obtained with **SecDec**. The evaluation of our analytic result relies on the use of **GiNaC** for the computation of the GPLs and on a one-dimensional integration for the cases where non-rational weights appear in the most external iteration, according to the eq. (3.29). As for the latter, we exploited the propriety of path-independence to choose simple paths (that avoid the singularities on the way from the basepoint to the chosen endpoints). Let us remark that in this work we did not focus on the efficiency of the numerical evaluation of the mixed Chen-Goncharov iterated integrals appearing in our analytic expression. This aspect, together with a study of the analytic properties of our solutions in the whole phase-space, requires a dedicated future investigation.

The analytic expressions of all the MIs are explicitly given in electronic form in ancillary files that can be obtained from the **arXiv** version of this paper.

6 Conclusions

In this article, we presented the calculation of the master integrals (MIs) needed for the virtual QCD×EW two-loop corrections to the Drell-Yan scattering processes,

$$q + \bar{q} \rightarrow l^- + l^+ , \quad q + \bar{q}' \rightarrow l^- + \bar{\nu} ,$$

for massless external particles. Besides the exchange of massless gauge bosons, such as gluons and photons, the relevant Feynman diagrams involve also the presence of W and Z propagators. Given the small difference between the masses of the W and Z bosons, in the diagrams containing both virtual particles at the same time, we performed a series expansion in the difference of the squared masses. Owing to this approximation, we distinguished three types of diagrams, according to the presence of massive internal lines: the no-mass type, the one-mass type, and the two-mass type, where all massive propagators, when occurring, contain the same mass value. The evaluations of the four point functions with one and two internal massive propagators are the main novel results of this communication.

To achieve it, we identified a basis of 49 MIs and evaluated them with the method of the differential equations. With the help of the Magnus exponential, the MIs were found to obey canonical systems of differential equations. Boundary conditions were imposed either by matching the solutions onto simpler integrals in special kinematic configurations, or by requiring the regularity of the solution at pseudothresholds. The canonical MIs were given as Taylor series around $d = 4$ space-time dimensions, up to order four, whose coefficients were given in terms of iterated integrals up to weight four. While the solution could be expressed, in full generality, in terms of Chen's iterated integrals, we adopted a mixed representation in terms of Chen-Goncharov iterated integrals, suitable for their numerical evaluation. Further studies concerning the analytic properties of the presented MIs in the

whole phase-space, and the optimization of their numerical evaluation will be the subject of a forthcoming publication.

Acknowledgments

We would like to thank Valery Yundin for his contribution during the early stages of this project. We thank Lorenzo Tancredi for clarifying discussions and Matthias Kerner for technical support with `SecDec`. Some of the algebraic manipulations required in this work were carried out with `FORM` [124]. The Feynman diagrams were generated by `FeynArts` [125, 126] and drawn with `Axodraw` [127]. The work of R.B. was partly supported by European Community Seventh Framework Programme FP7/2007-2013, under grant agreement N.302997. The work of P.M. and U.S. was supported by the Alexander von Humboldt Foundation, in the framework of the Sofja Kovalevskaja Award 2010, endowed by the German Federal Ministry of Education and Research. R.B. and S.D.V. would like to thank the Galileo Galilei Institute for Theoretical Physics for hospitality during the initial part of this work.

A Variables for the one-mass and two-mass integrals

In this section we discuss the domain of the variables employed in the analytic expressions of the MIs for the Drell-Yan process, both in the case with one massive propagator and in the case with two massive propagators.

A.1 One-mass type

For the evaluation of the one-mass MIs we simply rescale by the squared mass the Mandelstam invariants. All the analytic results are given in terms of two-dimensional generalized polylogarithms, functions of the variables

$$x = -\frac{s}{m^2}, \quad y = -\frac{t}{m^2}. \quad (\text{A.1})$$

In the Euclidean region $s, t < 0$. Therefore, if $m^2 > 0$, both x and y are real and positive. The analytic continuation to the other values of s and t , with $m^2 > 0$, requires the Feynman prescription on the invariants. In particular, in the physical region s becomes positive, with a positive vanishing imaginary part, $s + i0^+$. Accordingly, x is negative, with a negative vanishing imaginary part:

$$x \rightarrow -x' - i0^+, \quad (\text{A.2})$$

with

$$x' = \frac{s}{m^2} > 0. \quad (\text{A.3})$$

On the other hand, t is negative and ranges between $-s$ and 0, so that $0 < y < x'$. The extension to the case of complex mass, $m^2 \rightarrow m^2 - im\Gamma$, is straightforward.

The numeric evaluation of the MIs expressed in terms of GPLs of the variables x and y can be done in the whole (s, t, m^2) domain using the routines in [102] expressing our analytic formulas in terms of GPLs evaluated in 1 and giving the explicit imaginary part to the Mandelstam variables (see for instance [128]).

A.2 Two-mass type

For the evaluation of the two-mass MIs, see section 5, we find it convenient to introduce the reduced variables w and z defined by

$$-\frac{s}{m^2} = \frac{(1-w)^2}{w}, \quad -\frac{t}{m^2} = \frac{w(1+z)^2}{z(1+w)^2}. \quad (\text{A.4})$$

We note that the above mapping allows the evaluation of our results everywhere in the (s, t) plane, with the exception of the value $w = -1$ (corresponding to $s = 4m^2$). For that specific value of w , the t dependence in z gets lost by construction, and $z = -1$ independently of t . The evaluation of the solution at $s = 4m^2$ requires further investigations and it will be addressed in a forthcoming publication.

The arguments in the following sections rely on the assumption that $m^2 > 0$. Nevertheless, the whole discussion can be straightforwardly extended to the case of complex mass, $m^2 \rightarrow m^2 - im\Gamma$. For instance, it is easy to see that in the physical region, defined by $s > 0$ and $-s < t < 0$ (see section 2), the real and imaginary parts of (w, z) would differ from those in the zero-width case. Nevertheless, the sign of the imaginary parts will be preserved. Therefore the zero-width case would simply arise as a limit. Furthermore, in the presence of a non-zero width, the change of variables (A.4) is always well defined for any real s , thus circumventing the difficulty mentioned above.

A.2.1 Range of values for w

For w , defined by the first of eqs. (A.4), we choose the following root:

$$w = \frac{\sqrt{4m^2 - s - i0^+} - \sqrt{-s - i0^+}}{\sqrt{4m^2 - s - i0^+} + \sqrt{-s - i0^+}}, \quad (\text{A.5})$$

where we explicitly used the Feynman prescription $s + i0^+$.

1. If $s < 0$, we have positive w and $0 < w < 1$. In particular, when $s \rightarrow -\infty$, $w \rightarrow 0$, while for $s \rightarrow 0$, $w \rightarrow 1$.
2. If $0 < s < 4m^2$, w becomes a phase. In fact

$$w = \frac{\sqrt{4m^2 - s} + i\sqrt{s}}{\sqrt{4m^2 - s} - i\sqrt{s}} = e^{i\phi}, \quad (\text{A.6})$$

where

$$\phi = 2 \arctan \sqrt{\frac{s}{4m^2 - s}} \quad (\text{A.7})$$

and $0 < \phi < \pi$.

3. If $s > 4m^2$, w becomes negative (with a positive vanishing imaginary part)

$$w = -\frac{\sqrt{s} - \sqrt{s - 4m^2}}{\sqrt{s} + \sqrt{s - 4m^2}} = -w' + i0^+, \quad (\text{A.8})$$

and $1 > w' > 0$ when $4m^2 < s < +\infty$.

A.2.2 Range of values for z

The variable z depends both on s and t . In order to study the different regimes, we define the following function of s

$$\begin{aligned} t_* &\equiv -m^2 \frac{w}{(1+w)^2} \\ &= -\frac{m^4}{4m^2 - s}. \end{aligned} \quad (\text{A.9})$$

where the second equality follows from eq. (A.5). We also define the ratio

$$K \equiv \frac{t}{t_*}, \quad (\text{A.10})$$

so that the second of eqs. (A.4) reads

$$K = \frac{(1+z)^2}{z}. \quad (\text{A.11})$$

We choose the following root of the above equation

$$z = \frac{\sqrt{K} - \sqrt{K-4}}{\sqrt{K} + \sqrt{K-4}}. \quad (\text{A.12})$$

Note that eq. (A.12) contains square-roots of K and $K-4$. Therefore, in order to compute z when $K < 4$, we have to keep track of the vanishing imaginary parts of the quantities entering eq. (A.10). Region by region in the (s, t) plane, the correct sign of the vanishing imaginary part (if present) is determined by the Feynman prescription on s, t, u , i.e. $s + i0^+$ when $s > 0$, and likewise for t and u .

Depending on the value of K , we distinguish three cases (here we keep the prescription for the vanishing imaginary part of K arbitrary):

1. $K > 4$

All the square roots in eq. (A.12) are real, so z is real with $0 < z < 1$.

2. $0 < K < 4$

For a given prescription $K \pm i0^+$, one obtains from eq. (A.12)

$$z = \frac{\sqrt{K} \mp i\sqrt{4-K}}{\sqrt{K} \pm i\sqrt{4-K}}, \quad (\text{A.13})$$

which is solved by

$$z = e^{\mp i\psi}, \quad \psi = 2 \arctan \sqrt{\frac{4-K}{K}}, \quad 0 < \psi < \pi. \quad (\text{A.14})$$

3. $K < 0$

| | $t < -4 t_* $ | $-4 t_* < t < 0$ | $0 < t < t_* $ | $ t_* < t < 4 t_* $ | $t > 4 t_* $ |
|----------------|---------------|----------------------|-----------------|----------------------|--------------|
| $s < 0$ | z | $e^{-i\psi}$ | $-z' + i0^+$ | $-z' + i0^+$ | $-z' + i0^+$ |
| $0 < s < 4m^2$ | z | $\mathbf{e}^{i\psi}$ | $-z' + i0^+$ | $-z' - i0^+$ | $-z' - i0^+$ |
| $s > 4m^2$ | $-z' + i0^+$ | $-z' + i0^+$ | $e^{-i\psi}$ | $e^{-i\psi}$ | z |

Table 1. We show the solution for z in each region of the (s, t) plane, as in eqs. (A.12), (A.14), and (A.15). The boldface entries are the solutions in the regions that contain a part of the physical s -channel scattering region, $s > 0$ with $-s < t < 0$.

For a given prescription $K \pm i0^+$, one obtains from eq. (A.12)

$$\begin{aligned}
 z &= \frac{\sqrt{-|K| \pm i0^+} - \sqrt{-|K| - 4 \pm i0^+}}{\sqrt{-|K| \pm i0^+} + \sqrt{-|K| - 4 \pm i0^+}} \\
 &= \frac{\sqrt{|K|} - \sqrt{|K| + 4}}{\sqrt{|K|} + \sqrt{|K| + 4}} \mp i0^+ \\
 &\equiv -z' \mp i0^+,
 \end{aligned} \tag{A.15}$$

with $0 < z' < 1$.

Note that, since K is a function of s and t , each case can arise from multiple regions in the (s, t) plane. In table 1 we summarize the solution for z in the different regions of the (s, t) plane, by displaying also the appropriate sign for the $i0^+$ prescription (if a vanishing imaginary part is present).

B Two-loop $d\log$ -forms

In this appendix we give explicitly the coefficient matrices of the $d\log$ -forms, eq. (3.4), for the one-mass and the two-mass two-loop MIs, discussed respectively in sections 4 and 5.

B.1 One-mass

For the one-mass case at the two-loop order, the $d\log$ -form is

$$\begin{aligned}
 d\mathbb{A} &= \mathbb{M}_1 d\log(1+x) + \mathbb{M}_2 d\log(x) + \mathbb{M}_3 d\log(y) \\
 &\quad + \mathbb{M}_4 d\log(1-y) + \mathbb{M}_5 d\log(x+y) + \mathbb{M}_6 d\log(x+y+xy)
 \end{aligned} \tag{B.1}$$

JHEP09(2016)091

(B.2)

(B.3)

[illegible]

[illegible]

[illegible]

[illegible]

[illegible]

[illegible]

[illegible]

[illegible]

[illegible]

[illegible]

- [7] G. Heinrich, T. Huber, D.A. Kosower and V.A. Smirnov, *Nine-propagator master integrals for massless three-loop form factors*, *Phys. Lett. B* **678** (2009) 359 [[arXiv:0902.3512](#)] [[INSPIRE](#)].
- [8] P.A. Baikov, K.G. Chetyrkin, A.V. Smirnov, V.A. Smirnov and M. Steinhauser, *Quark and gluon form factors to three loops*, *Phys. Rev. Lett.* **102** (2009) 212002 [[arXiv:0902.3519](#)] [[INSPIRE](#)].
- [9] R.N. Lee, A.V. Smirnov and V.A. Smirnov, *Analytic results for massless three-loop form factors*, *JHEP* **04** (2010) 020 [[arXiv:1001.2887](#)] [[INSPIRE](#)].
- [10] T. Gehrmann, E.W.N. Glover, T. Huber, N. Ikizlerli and C. Studerus, *Calculation of the quark and gluon form factors to three loops in QCD*, *JHEP* **06** (2010) 094 [[arXiv:1004.3653](#)] [[INSPIRE](#)].
- [11] J.R. Andersen et al., *Les Houches 2013 — physics at TeV colliders: Standard Model working group report*, [arXiv:1405.1067](#) [[INSPIRE](#)].
- [12] G. Altarelli, R.K. Ellis and G. Martinelli, *Large perturbative corrections to the Drell-Yan process in QCD*, *Nucl. Phys. B* **157** (1979) 461 [[INSPIRE](#)].
- [13] G. Altarelli, R.K. Ellis, M. Greco and G. Martinelli, *Vector boson production at colliders: a theoretical reappraisal*, *Nucl. Phys. B* **246** (1984) 12 [[INSPIRE](#)].
- [14] T. Matsuura, S.C. van der Marck and W.L. van Neerven, *The calculation of the second order soft and virtual contributions to the Drell-Yan cross-section*, *Nucl. Phys. B* **319** (1989) 570 [[INSPIRE](#)].
- [15] R. Hamberg, W.L. van Neerven and T. Matsuura, *A complete calculation of the order α_s^2 correction to the Drell-Yan K factor*, *Nucl. Phys. B* **359** (1991) 343 [*Erratum ibid.* **B 644** (2002) 403] [[INSPIRE](#)].
- [16] G.F. Sterman, *Summation of large corrections to short distance hadronic cross-sections*, *Nucl. Phys. B* **281** (1987) 310 [[INSPIRE](#)].
- [17] S. Catani and L. Trentadue, *Resummation of the QCD perturbative series for hard processes*, *Nucl. Phys. B* **327** (1989) 323 [[INSPIRE](#)].
- [18] S. Catani and L. Trentadue, *Comment on QCD exponentiation at large x*, *Nucl. Phys. B* **353** (1991) 183 [[INSPIRE](#)].
- [19] S. Moch and A. Vogt, *Higher-order soft corrections to lepton pair and Higgs boson production*, *Phys. Lett. B* **631** (2005) 48 [[hep-ph/0508265](#)] [[INSPIRE](#)].
- [20] D. Wackeroth and W. Hollik, *Electroweak radiative corrections to resonant charged gauge boson production*, *Phys. Rev. D* **55** (1997) 6788 [[hep-ph/9606398](#)] [[INSPIRE](#)].
- [21] U. Baur, S. Keller and W.K. Sakumoto, *QED radiative corrections to Z boson production and the forward backward asymmetry at hadron colliders*, *Phys. Rev. D* **57** (1998) 199 [[hep-ph/9707301](#)] [[INSPIRE](#)].
- [22] R.K. Ellis, G. Martinelli and R. Petronzio, *Lepton pair production at large transverse momentum in second order QCD*, *Nucl. Phys. B* **211** (1983) 106 [[INSPIRE](#)].
- [23] P.B. Arnold and M.H. Reno, *The complete computation of high p_T W and Z production in 2nd order QCD*, *Nucl. Phys. B* **319** (1989) 37 [*Erratum ibid.* **B 330** (1990) 284] [[INSPIRE](#)].

- [24] R.J. Gonsalves, J. Pawłowski and C.-F. Wai, *QCD radiative corrections to electroweak boson production at large transverse momentum in hadron collisions*, *Phys. Rev. D* **40** (1989) 2245 [[INSPIRE](#)].
- [25] F.T. Brandt, G. Kramer and S.-L. Nyeo, *W, Z plus jet production at $p\bar{p}$ colliders*, *Int. J. Mod. Phys. A* **6** (1991) 3973 [[INSPIRE](#)].
- [26] W.T. Giele, E.W.N. Glover and D.A. Kosower, *Higher order corrections to jet cross-sections in hadron colliders*, *Nucl. Phys. B* **403** (1993) 633 [[hep-ph/9302225](#)] [[INSPIRE](#)].
- [27] L.J. Dixon, Z. Kunszt and A. Signer, *Helicity amplitudes for $O(\alpha_s)$ production of W^+W^- , $W^\pm Z$, ZZ , $W^\pm\gamma$, or $Z\gamma$ pairs at hadron colliders*, *Nucl. Phys. B* **531** (1998) 3 [[hep-ph/9803250](#)] [[INSPIRE](#)].
- [28] J.H. Kuhn, A. Kulesza, S. Pozzorini and M. Schulze, *Logarithmic electroweak corrections to hadronic $Z + 1$ jet production at large transverse momentum*, *Phys. Lett. B* **609** (2005) 277 [[hep-ph/0408308](#)] [[INSPIRE](#)].
- [29] A. Denner, S. Dittmaier, T. Kasprzik and A. Muck, *Electroweak corrections to $W +$ jet hadroproduction including leptonic W -boson decays*, *JHEP* **08** (2009) 075 [[arXiv:0906.1656](#)] [[INSPIRE](#)].
- [30] A. Denner, S. Dittmaier, T. Kasprzik and A. Muck, *Electroweak corrections to dilepton + jet production at hadron colliders*, *JHEP* **06** (2011) 069 [[arXiv:1103.0914](#)] [[INSPIRE](#)].
- [31] S. Kallweit, J.M. Lindert, P. Maierhöfer, S. Pozzorini and M. Schönherr, *NLO electroweak automation and precise predictions for $W +$ multijet production at the LHC*, *JHEP* **04** (2015) 012 [[arXiv:1412.5157](#)] [[INSPIRE](#)].
- [32] S. Kallweit, J.M. Lindert, P. Maierhofer, S. Pozzorini and M. Schönherr, *NLO QCD+EW predictions for $V +$ jets including off-shell vector-boson decays and multijet merging*, *JHEP* **04** (2016) 021 [[arXiv:1511.08692](#)] [[INSPIRE](#)].
- [33] T. Gehrmann and L. Tancredi, *Two-loop QCD helicity amplitudes for $q\bar{q} \rightarrow W^\pm\gamma$ and $q\bar{q} \rightarrow Z^0\gamma$* , *JHEP* **02** (2012) 004 [[arXiv:1112.1531](#)] [[INSPIRE](#)].
- [34] P.B. Arnold and R.P. Kauffman, *W and Z production at next-to-leading order: from large q_T to small*, *Nucl. Phys. B* **349** (1991) 381 [[INSPIRE](#)].
- [35] C. Balázs, J.-W. Qiu and C.P. Yuan, *Effects of QCD resummation on distributions of leptons from the decay of electroweak vector bosons*, *Phys. Lett. B* **355** (1995) 548 [[hep-ph/9505203](#)] [[INSPIRE](#)].
- [36] C. Balázs and C.P. Yuan, *Soft gluon effects on lepton pairs at hadron colliders*, *Phys. Rev. D* **56** (1997) 5558 [[hep-ph/9704258](#)] [[INSPIRE](#)].
- [37] R.K. Ellis, D.A. Ross and S. Veseli, *Vector boson production in hadronic collisions*, *Nucl. Phys. B* **503** (1997) 309 [[hep-ph/9704239](#)] [[INSPIRE](#)].
- [38] R.K. Ellis and S. Veseli, *W and Z transverse momentum distributions: resummation in q_T space*, *Nucl. Phys. B* **511** (1998) 649 [[hep-ph/9706526](#)] [[INSPIRE](#)].
- [39] J.-W. Qiu and X.-F. Zhang, *QCD prediction for heavy boson transverse momentum distributions*, *Phys. Rev. Lett.* **86** (2001) 2724 [[hep-ph/0012058](#)] [[INSPIRE](#)].
- [40] J.-W. Qiu and X.-F. Zhang, *Role of the nonperturbative input in QCD resummed Drell-Yan Q_T distributions*, *Phys. Rev. D* **63** (2001) 114011 [[hep-ph/0012348](#)] [[INSPIRE](#)].

- [41] A. Kulesza and W.J. Stirling, *Soft gluon resummation in transverse momentum space for electroweak boson production at hadron colliders*, *Eur. Phys. J. C* **20** (2001) 349 [[hep-ph/0103089](#)] [[INSPIRE](#)].
- [42] A. Kulesza, G.F. Sterman and W. Vogelsang, *Joint resummation in electroweak boson production*, *Phys. Rev. D* **66** (2002) 014011 [[hep-ph/0202251](#)] [[INSPIRE](#)].
- [43] F. Landry, R. Brock, P.M. Nadolsky and C.P. Yuan, *Tevatron Run-1 Z boson data and Collins-Soper-Sterman resummation formalism*, *Phys. Rev. D* **67** (2003) 073016 [[hep-ph/0212159](#)] [[INSPIRE](#)].
- [44] G. Bozzi, S. Catani, G. Ferrera, D. de Florian and M. Grazzini, *Production of Drell-Yan lepton pairs in hadron collisions: transverse-momentum resummation at next-to-next-to-leading logarithmic accuracy*, *Phys. Lett. B* **696** (2011) 207 [[arXiv:1007.2351](#)] [[INSPIRE](#)].
- [45] C. Anastasiou, L.J. Dixon, K. Melnikov and F. Petriello, *Dilepton rapidity distribution in the Drell-Yan process at NNLO in QCD*, *Phys. Rev. Lett.* **91** (2003) 182002 [[hep-ph/0306192](#)] [[INSPIRE](#)].
- [46] S. Dittmaier and M. Krämer, *Electroweak radiative corrections to W boson production at hadron colliders*, *Phys. Rev. D* **65** (2002) 073007 [[hep-ph/0109062](#)] [[INSPIRE](#)].
- [47] S. Dittmaier and M. Huber, *Radiative corrections to the neutral-current Drell-Yan process in the Standard Model and its minimal supersymmetric extension*, *JHEP* **01** (2010) 060 [[arXiv:0911.2329](#)] [[INSPIRE](#)].
- [48] A. Arbuzov et al., *One-loop corrections to the Drell-Yan process in SANC. I. The charged current case*, *Eur. Phys. J. C* **46** (2006) 407 [*Erratum ibid.* **C 50** (2007) 505] [[hep-ph/0506110](#)] [[INSPIRE](#)].
- [49] A. Arbuzov et al., *One-loop corrections to the Drell-Yan process in SANC. II. The neutral current case*, *Eur. Phys. J. C* **54** (2008) 451 [[arXiv:0711.0625](#)] [[INSPIRE](#)].
- [50] U. Baur, S. Keller and D. Wackeroth, *Electroweak radiative corrections to W boson production in hadronic collisions*, *Phys. Rev. D* **59** (1999) 013002 [[hep-ph/9807417](#)] [[INSPIRE](#)].
- [51] U. Baur, O. Brein, W. Hollik, C. Schappacher and D. Wackeroth, *Electroweak radiative corrections to neutral current Drell-Yan processes at hadron colliders*, *Phys. Rev. D* **65** (2002) 033007 [[hep-ph/0108274](#)] [[INSPIRE](#)].
- [52] U. Baur and D. Wackeroth, *Electroweak radiative corrections to $p\bar{p} \rightarrow W^\pm \rightarrow \ell^\pm \nu$ beyond the pole approximation*, *Phys. Rev. D* **70** (2004) 073015 [[hep-ph/0405191](#)] [[INSPIRE](#)].
- [53] S. Alioli, P. Nason, C. Oleari and E. Re, *NLO vector-boson production matched with shower in POWHEG*, *JHEP* **07** (2008) 060 [[arXiv:0805.4802](#)] [[INSPIRE](#)].
- [54] L. Barze, G. Montagna, P. Nason, O. Nicrosini and F. Piccinini, *Implementation of electroweak corrections in the POWHEG BOX: single W production*, *JHEP* **04** (2012) 037 [[arXiv:1202.0465](#)] [[INSPIRE](#)].
- [55] L. Barze, G. Montagna, P. Nason, O. Nicrosini, F. Piccinini and A. Vicini, *Neutral current Drell-Yan with combined QCD and electroweak corrections in the POWHEG BOX*, *Eur. Phys. J. C* **73** (2013) 2474 [[arXiv:1302.4606](#)] [[INSPIRE](#)].

- [56] C. Bernaciak and D. Wackerroth, *Combining NLO QCD and electroweak radiative corrections to W boson production at hadron colliders in the POWHEG framework*, *Phys. Rev. D* **85** (2012) 093003 [[arXiv:1201.4804](#)] [[INSPIRE](#)].
- [57] S. Frixione and B.R. Webber, *Matching NLO QCD computations and parton shower simulations*, *JHEP* **06** (2002) 029 [[hep-ph/0204244](#)] [[INSPIRE](#)].
- [58] S. Frixione, P. Nason and C. Oleari, *Matching NLO QCD computations with parton shower simulations: the POWHEG method*, *JHEP* **11** (2007) 070 [[arXiv:0709.2092](#)] [[INSPIRE](#)].
- [59] C.M. Carloni Calame, G. Montagna, O. Nicrosini and M. Treccani, *Higher order QED corrections to W boson mass determination at hadron colliders*, *Phys. Rev. D* **69** (2004) 037301 [[hep-ph/0303102](#)] [[INSPIRE](#)].
- [60] C.M. Carloni Calame, S. Jadach, G. Montagna, O. Nicrosini and W. Placzek, *Comparisons of the Monte Carlo programs HORACE and WINHAC for single W boson production at hadron colliders*, *Acta Phys. Polon. B* **35** (2004) 1643 [[hep-ph/0402235](#)] [[INSPIRE](#)].
- [61] C.M. Carloni Calame, G. Montagna, O. Nicrosini and M. Treccani, *Multiple photon corrections to the neutral-current Drell-Yan process*, *JHEP* **05** (2005) 019 [[hep-ph/0502218](#)] [[INSPIRE](#)].
- [62] C.M. Carloni Calame, G. Montagna, O. Nicrosini and A. Vicini, *Precision electroweak calculation of the charged current Drell-Yan process*, *JHEP* **12** (2006) 016 [[hep-ph/0609170](#)] [[INSPIRE](#)].
- [63] C.M. Carloni Calame, G. Montagna, O. Nicrosini and A. Vicini, *Precision electroweak calculation of the production of a high transverse-momentum lepton pair at hadron colliders*, *JHEP* **10** (2007) 109 [[arXiv:0710.1722](#)] [[INSPIRE](#)].
- [64] P. Golonka and Z. Was, *PHOTOS Monte Carlo: a precision tool for QED corrections in Z and W decays*, *Eur. Phys. J. C* **45** (2006) 97 [[hep-ph/0506026](#)] [[INSPIRE](#)].
- [65] D. Bardin, S. Bondarenko, S. Jadach, L. Kalinovskaya and W. Placzek, *Implementation of SANC EW corrections in WINHAC Monte Carlo generator*, *Acta Phys. Polon. B* **40** (2009) 75 [[arXiv:0806.3822](#)] [[INSPIRE](#)].
- [66] W. Placzek and S. Jadach, *Multiphoton radiation in leptonic W boson decays*, *Eur. Phys. J. C* **29** (2003) 325 [[hep-ph/0302065](#)] [[INSPIRE](#)].
- [67] W. Placzek, S. Jadach and M.W. Krasny, *Drell-Yan processes with WINHAC*, *Acta Phys. Polon. B* **44** (2013) 2171 [[arXiv:1310.5994](#)] [[INSPIRE](#)].
- [68] E. Barberio, B. van Eijk and Z. Was, *PHOTOS: a universal Monte Carlo for QED radiative corrections in decays*, *Comput. Phys. Commun.* **66** (1991) 115 [[INSPIRE](#)].
- [69] E. Barberio and Z. Was, *PHOTOS: a universal Monte Carlo for QED radiative corrections. Version 2.0*, *Comput. Phys. Commun.* **79** (1994) 291 [[INSPIRE](#)].
- [70] K. Melnikov and F. Petriello, *The W boson production cross section at the LHC through $O(\alpha_s^2)$* , *Phys. Rev. Lett.* **96** (2006) 231803 [[hep-ph/0603182](#)] [[INSPIRE](#)].
- [71] R. Gavin, Y. Li, F. Petriello and S. Quackenbush, *W physics at the LHC with FEWZ 2.1*, *Comput. Phys. Commun.* **184** (2013) 208 [[arXiv:1201.5896](#)] [[INSPIRE](#)].
- [72] Y. Li and F. Petriello, *Combining QCD and electroweak corrections to dilepton production in FEWZ*, *Phys. Rev. D* **86** (2012) 094034 [[arXiv:1208.5967](#)] [[INSPIRE](#)].

- [73] S. Catani and M. Grazzini, *An NNLO subtraction formalism in hadron collisions and its application to Higgs boson production at the LHC*, *Phys. Rev. Lett.* **98** (2007) 222002 [[hep-ph/0703012](#)] [[INSPIRE](#)].
- [74] S. Catani, L. Cieri, G. Ferrera, D. de Florian and M. Grazzini, *Vector boson production at hadron colliders: a fully exclusive QCD calculation at NNLO*, *Phys. Rev. Lett.* **103** (2009) 082001 [[arXiv:0903.2120](#)] [[INSPIRE](#)].
- [75] A. Karlberg, E. Re and G. Zanderighi, *NNLOPS accurate Drell-Yan production*, *JHEP* **09** (2014) 134 [[arXiv:1407.2940](#)] [[INSPIRE](#)].
- [76] S. Höche, Y. Li and S. Prestel, *Drell-Yan lepton pair production at NNLO QCD with parton showers*, *Phys. Rev. D* **91** (2015) 074015 [[arXiv:1405.3607](#)] [[INSPIRE](#)].
- [77] S. Alioli, C.W. Bauer, C. Berggren, F.J. Tackmann and J.R. Walsh, *Drell-Yan production at NNLL'+NNLO matched to parton showers*, *Phys. Rev. D* **92** (2015) 094020 [[arXiv:1508.01475](#)] [[INSPIRE](#)].
- [78] W.B. Kilgore and C. Sturm, *Two-loop virtual corrections to Drell-Yan production at order $\alpha_s\alpha^3$* , *Phys. Rev. D* **85** (2012) 033005 [[arXiv:1107.4798](#)] [[INSPIRE](#)].
- [79] A. Kotikov, J.H. Kuhn and O. Veretin, *Two-loop formfactors in theories with mass gap and Z-boson production*, *Nucl. Phys. B* **788** (2008) 47 [[hep-ph/0703013](#)] [[INSPIRE](#)].
- [80] S. Dittmaier, A. Huss and C. Schwinn, *Mixed QCD-electroweak $O(\alpha_s\alpha)$ corrections to Drell-Yan processes in the resonance region: pole approximation and non-factorizable corrections*, *Nucl. Phys. B* **885** (2014) 318 [[arXiv:1403.3216](#)] [[INSPIRE](#)].
- [81] S. Dittmaier, A. Huss and C. Schwinn, *Dominant mixed QCD-electroweak $O(\alpha_s\alpha)$ corrections to Drell-Yan processes in the resonance region*, *Nucl. Phys. B* **904** (2016) 216 [[arXiv:1511.08016](#)] [[INSPIRE](#)].
- [82] R. Bonciani, *Two-loop mixed QCD-EW virtual corrections to the Drell-Yan production of Z and W bosons*, *PoS(EPS-HEP2011)* 365 [[INSPIRE](#)].
- [83] C. Studerus, *Reduze-Feynman integral reduction in C++*, *Comput. Phys. Commun.* **181** (2010) 1293 [[arXiv:0912.2546](#)] [[INSPIRE](#)].
- [84] A. von Manteuffel and C. Studerus, *Reduze 2 — distributed Feynman integral reduction*, [arXiv:1201.4330](#) [[INSPIRE](#)].
- [85] A.V. Kotikov, *Differential equations method: new technique for massive Feynman diagrams calculation*, *Phys. Lett. B* **254** (1991) 158 [[INSPIRE](#)].
- [86] E. Remiddi, *Differential equations for Feynman graph amplitudes*, *Nuovo Cim. A* **110** (1997) 1435 [[hep-th/9711188](#)] [[INSPIRE](#)].
- [87] T. Gehrmann and E. Remiddi, *Differential equations for two loop four point functions*, *Nucl. Phys. B* **580** (2000) 485 [[hep-ph/9912329](#)] [[INSPIRE](#)].
- [88] M. Argeri and P. Mastrolia, *Feynman diagrams and differential equations*, *Int. J. Mod. Phys. A* **22** (2007) 4375 [[arXiv:0707.4037](#)] [[INSPIRE](#)].
- [89] J.M. Henn, *Lectures on differential equations for Feynman integrals*, *J. Phys. A* **48** (2015) 153001 [[arXiv:1412.2296](#)] [[INSPIRE](#)].
- [90] J.M. Henn, *Multiloop integrals in dimensional regularization made simple*, *Phys. Rev. Lett.* **110** (2013) 251601 [[arXiv:1304.1806](#)] [[INSPIRE](#)].

- [91] M. Argeri et al., *Magnus and Dyson series for master integrals*, *JHEP* **03** (2014) 082 [[arXiv:1401.2979](#)] [[INSPIRE](#)].
- [92] S. Di Vita, P. Mastrolia, U. Schubert and V. Yundin, *Three-loop master integrals for ladder-box diagrams with one massive leg*, *JHEP* **09** (2014) 148 [[arXiv:1408.3107](#)] [[INSPIRE](#)].
- [93] J.M. Henn, A.V. Smirnov and V.A. Smirnov, *Evaluating single-scale and/or non-planar diagrams by differential equations*, *JHEP* **03** (2014) 088 [[arXiv:1312.2588](#)] [[INSPIRE](#)].
- [94] T. Gehrmann, A. von Manteuffel, L. Tancredi and E. Weihs, *The two-loop master integrals for $q\bar{q} \rightarrow VV$* , *JHEP* **06** (2014) 032 [[arXiv:1404.4853](#)] [[INSPIRE](#)].
- [95] R.N. Lee, *Reducing differential equations for multiloop master integrals*, *JHEP* **04** (2015) 108 [[arXiv:1411.0911](#)] [[INSPIRE](#)].
- [96] A. Goncharov, *Polylogarithms in arithmetic and geometry*, in *Proceedings of the International Congress of Mathematicians* **1,2**, (1995), pg. 374.
- [97] A.B. Goncharov, *Multiple polylogarithms and mixed Tate motives*, [math/0103059](#) [[INSPIRE](#)].
- [98] V.A. Smirnov, *Analytical result for dimensionally regularized massless on shell double box*, *Phys. Lett. B* **460** (1999) 397 [[hep-ph/9905323](#)] [[INSPIRE](#)].
- [99] J.B. Tausk, *Nonplanar massless two loop Feynman diagrams with four on-shell legs*, *Phys. Lett. B* **469** (1999) 225 [[hep-ph/9909506](#)] [[INSPIRE](#)].
- [100] C. Anastasiou, T. Gehrmann, C. Oleari, E. Remiddi and J.B. Tausk, *The tensor reduction and master integrals of the two loop massless crossed box with lightlike legs*, *Nucl. Phys. B* **580** (2000) 577 [[hep-ph/0003261](#)] [[INSPIRE](#)].
- [101] S. Caron-Huot and J.M. Henn, *Iterative structure of finite loop integrals*, *JHEP* **06** (2014) 114 [[arXiv:1404.2922](#)] [[INSPIRE](#)].
- [102] J. Vollinga and S. Weinzierl, *Numerical evaluation of multiple polylogarithms*, *Comput. Phys. Commun.* **167** (2005) 177 [[hep-ph/0410259](#)] [[INSPIRE](#)].
- [103] F.V. Tkachov, *A theorem on analytical calculability of four loop renormalization group functions*, *Phys. Lett. B* **100** (1981) 65 [[INSPIRE](#)].
- [104] K.G. Chetyrkin and F.V. Tkachov, *Integration by parts: the algorithm to calculate β -functions in 4 loops*, *Nucl. Phys. B* **192** (1981) 159 [[INSPIRE](#)].
- [105] C. Anastasiou and A. Lazopoulos, *Automatic integral reduction for higher order perturbative calculations*, *JHEP* **07** (2004) 046 [[hep-ph/0404258](#)] [[INSPIRE](#)].
- [106] A.V. Smirnov, *Algorithm FIRE – Feynman Integral REduction*, *JHEP* **10** (2008) 107 [[arXiv:0807.3243](#)] [[INSPIRE](#)].
- [107] A.V. Smirnov and V.A. Smirnov, *FIRE4, LiteRed and accompanying tools to solve integration by parts relations*, *Comput. Phys. Commun.* **184** (2013) 2820 [[arXiv:1302.5885](#)] [[INSPIRE](#)].
- [108] A.V. Smirnov, *FIRE5: a C++ implementation of Feynman Integral REduction*, *Comput. Phys. Commun.* **189** (2015) 182 [[arXiv:1408.2372](#)] [[INSPIRE](#)].
- [109] R.N. Lee, *Presenting LiteRed: a tool for the Loop InTEgrals REDuction*, [arXiv:1212.2685](#) [[INSPIRE](#)].

- [110] R.N. Lee, *LiteRed 1.4: a powerful tool for reduction of multiloop integrals*, *J. Phys. Conf. Ser.* **523** (2014) 012059 [[arXiv:1310.1145](#)] [[INSPIRE](#)].
- [111] J. Fleischer, A.V. Kotikov and O.L. Veretin, *Analytic two loop results for selfenergy type and vertex type diagrams with one nonzero mass*, *Nucl. Phys. B* **547** (1999) 343 [[hep-ph/9808242](#)] [[INSPIRE](#)].
- [112] U. Aglietti and R. Bonciani, *Master integrals with one massive propagator for the two loop electroweak form-factor*, *Nucl. Phys. B* **668** (2003) 3 [[hep-ph/0304028](#)] [[INSPIRE](#)].
- [113] R. Bonciani, P. Mastrolia and E. Remiddi, *Master integrals for the two loop QCD virtual corrections to the forward backward asymmetry*, *Nucl. Phys. B* **690** (2004) 138 [[hep-ph/0311145](#)] [[INSPIRE](#)].
- [114] U. Aglietti and R. Bonciani, *Master integrals with 2 and 3 massive propagators for the 2 loop electroweak form-factor — planar case*, *Nucl. Phys. B* **698** (2004) 277 [[hep-ph/0401193](#)] [[INSPIRE](#)].
- [115] U. Aglietti, R. Bonciani, G. Degrossi and A. Vicini, *Master integrals for the two-loop light fermion contributions to $gg \rightarrow H$ and $H \rightarrow \gamma\gamma$* , *Phys. Lett. B* **600** (2004) 57 [[hep-ph/0407162](#)] [[INSPIRE](#)].
- [116] W. Magnus, *On the exponential solution of differential equations for a linear operator*, *Commun. Pure Appl. Math.* **7** (1954) 649 [[INSPIRE](#)].
- [117] K.-T. Chen, *Iterated path integrals*, *Bull. Amer. Math. Soc.* **83** (1977) 831 [[INSPIRE](#)].
- [118] F.C.S. Brown, *Multiple zeta values and periods of moduli spaces $\overline{\mathcal{M}}_{0,n}(\mathbb{R})$* , *Annales Sci. Ecole Norm. Sup.* **42** (2009) 371 [[math/0606419](#)] [[INSPIRE](#)].
- [119] F.C.S. Brown, *Iterated integrals in quantum field theory*, IHES, (2013) [[INSPIRE](#)].
- [120] D.J. Broadhurst, *Massive three-loop Feynman diagrams reducible to SC^* primitives of algebras of the sixth root of unity*, *Eur. Phys. J. C* **8** (1999) 311 [[hep-th/9803091](#)] [[INSPIRE](#)].
- [121] J. Zhao, *Standard relations of multiple polylogarithm values at roots of unity*, [arXiv:0707.1459](#).
- [122] F. Moriello, *Linearization and symmetrization of generalized harmonic polylogarithms*, *Master Thesis*, University of Rome “La Sapienza”, Rome Italy April 2013.
- [123] J.M. Henn, A.V. Smirnov and V.A. Smirnov, *Evaluating multiple polylogarithm values at sixth roots of unity up to weight six*, [arXiv:1512.08389](#) [[INSPIRE](#)].
- [124] J. Kuipers, T. Ueda, J.A.M. Vermaseren and J. Vollinga, *FORM version 4.0*, *Comput. Phys. Commun.* **184** (2013) 1453 [[arXiv:1203.6543](#)] [[INSPIRE](#)].
- [125] J. Kublbeck, M. Böhm and A. Denner, *Feyn Arts: computer algebraic generation of Feynman graphs and amplitudes*, *Comput. Phys. Commun.* **60** (1990) 165 [[INSPIRE](#)].
- [126] T. Hahn, *Generating Feynman diagrams and amplitudes with FeynArts 3*, *Comput. Phys. Commun.* **140** (2001) 418 [[hep-ph/0012260](#)] [[INSPIRE](#)].
- [127] J.A.M. Vermaseren, *Axodraw*, *Comput. Phys. Commun.* **83** (1994) 45 [[INSPIRE](#)].
- [128] R. Bonciani, G. Degrossi and A. Vicini, *On the generalized harmonic polylogarithms of one complex variable*, *Comput. Phys. Commun.* **182** (2011) 1253 [[arXiv:1007.1891](#)] [[INSPIRE](#)].